Potential of multiwavelength lidars for particles characterization: expectations and challenges

Igor Veselovskii

Physics Instrumentation Center, Russia

MOTIVATION

There is a current concern about the effects of atmospheric aerosol on climate

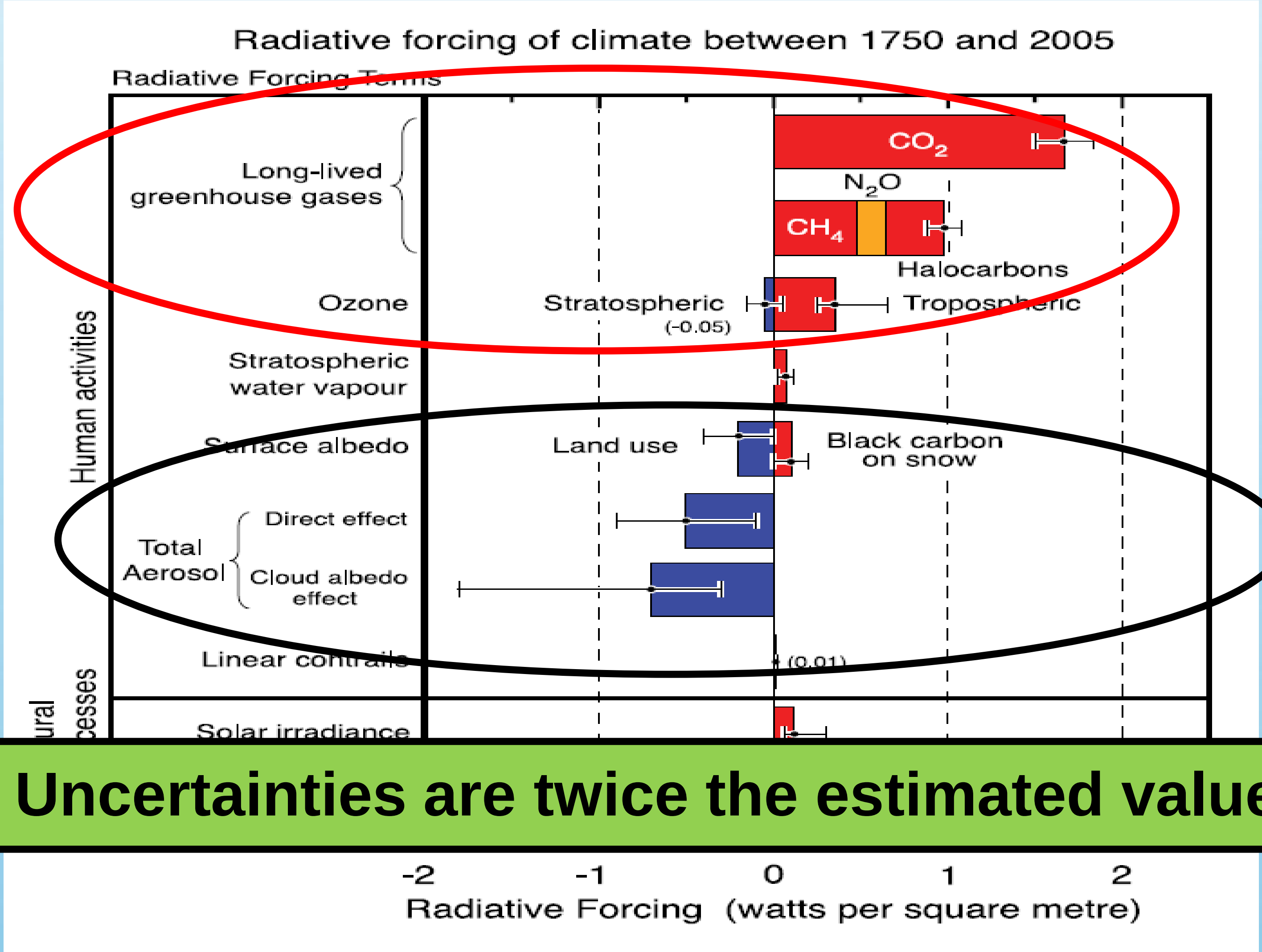

Uncertainties are twice the estimated value

Potential of multiwavelength lidar

MW Raman (HSRL) lidar provides backscattering β, extinction α and depolarization δ at multiple wavelengths. From these we can obtain:

Intensive parameters: lidar ratios, Angstrom exponent, depolarization → Aerosol classification

Inversion ↓

Particle size, concentration, refractive index, SSA → Microphysical parameters

Time series ↓

Height -temporal distributions of particle parameters → Dynamics

Configuration of lidar for ACE mission is still the subject of discussions.

Multiwavelength HSRL

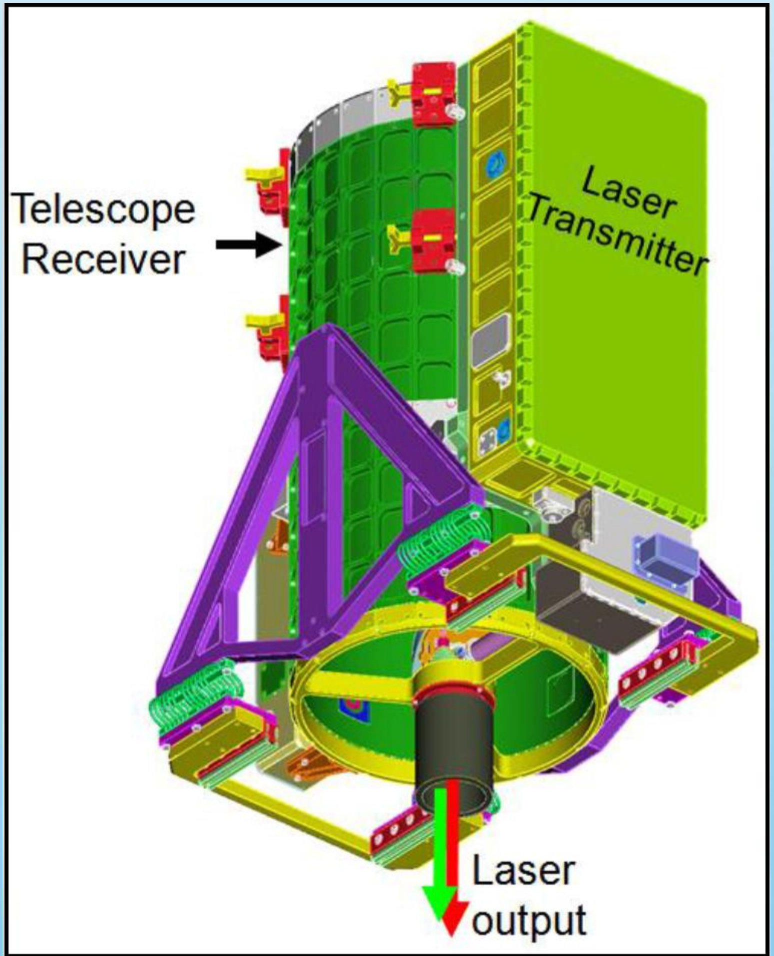

- Backscatter at 3 wavelengths (3β) : 355, 532, 1064 nm
- Extinction at 2 wavelengths (2α) : 355, 532 nm
- Depolarization at 355, 532, and 1064 (dust and contrails/cirrus applications)

  - It is always desirable to reduce the number of channels.
  - Retrieval should be tolerant to the input data noise

From Chris Hostetler, LARC

High Spectral Resolution Lidar (HSRL) Technique Iodine Vapor Filter Implementation)

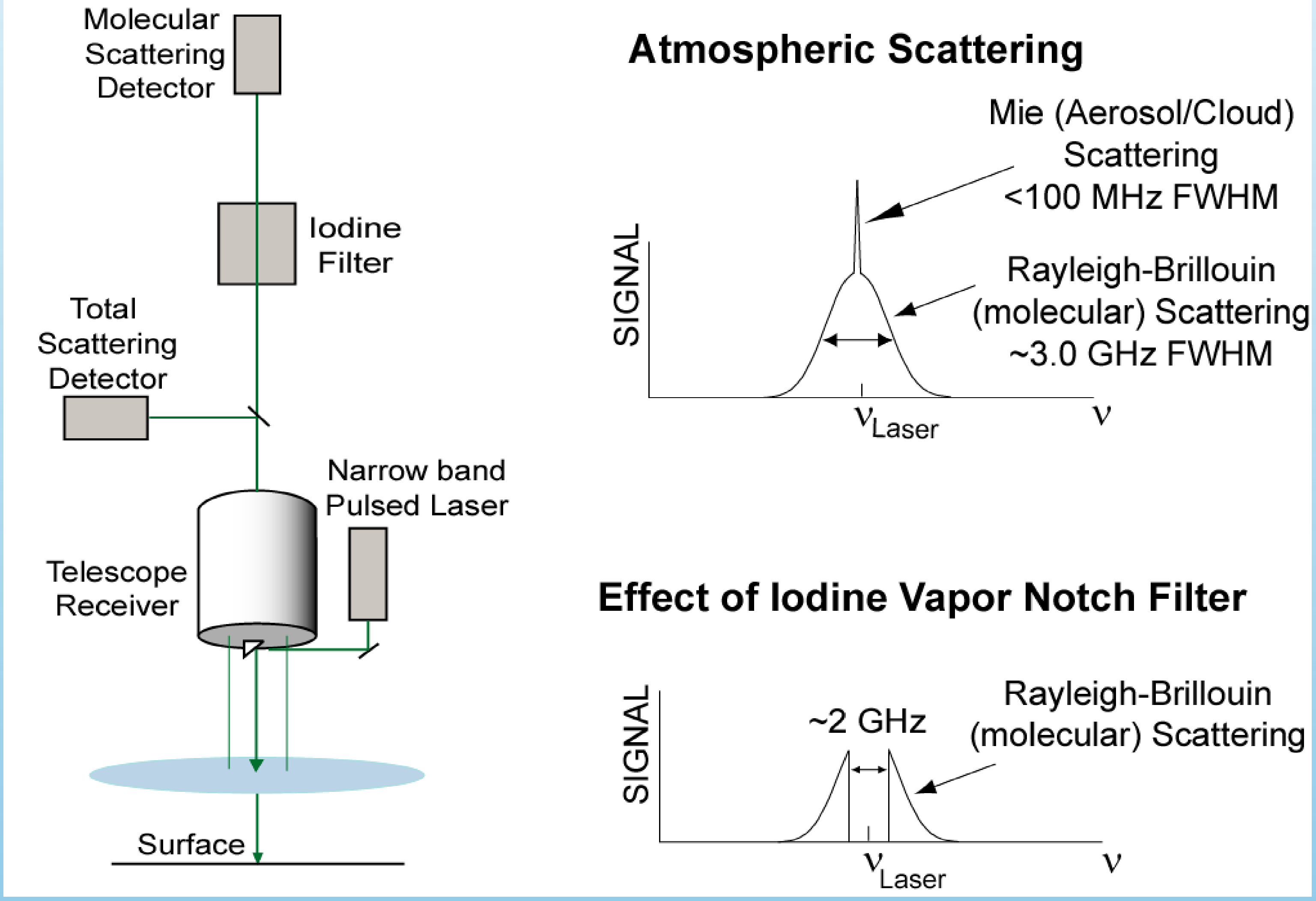

Challenges of multiwavelength technique

- Small number of data
- Unknown complex refractive index and particle size distribution
- Significant input errors (up to 20%)
- Necessity to process large volume of data
- Particle nonsphericity
- Spectral and size dependence of complex refractive index
- Mixture of particles

Two approaches to inversion

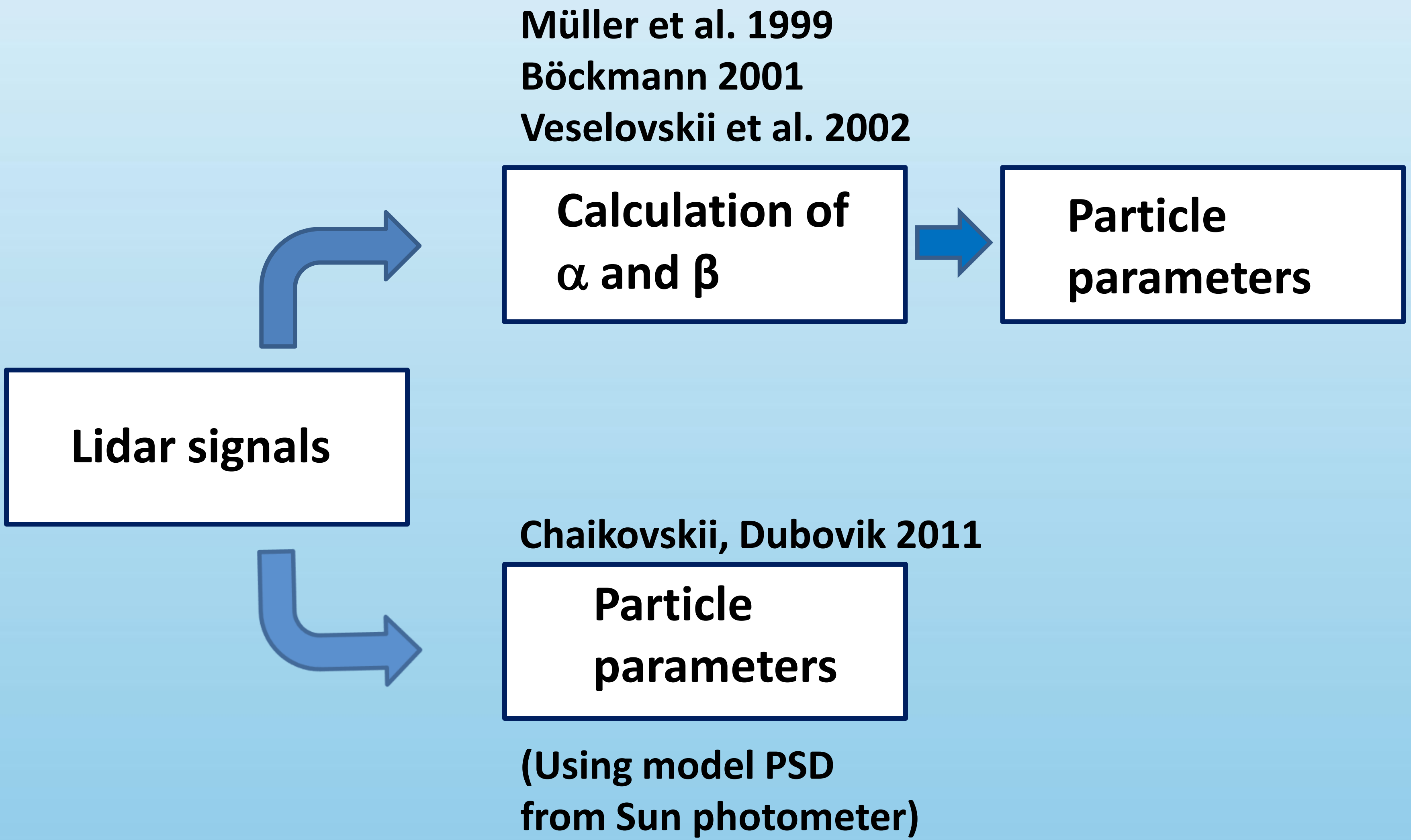

LIRIC becomes popular and useful within EARLINET

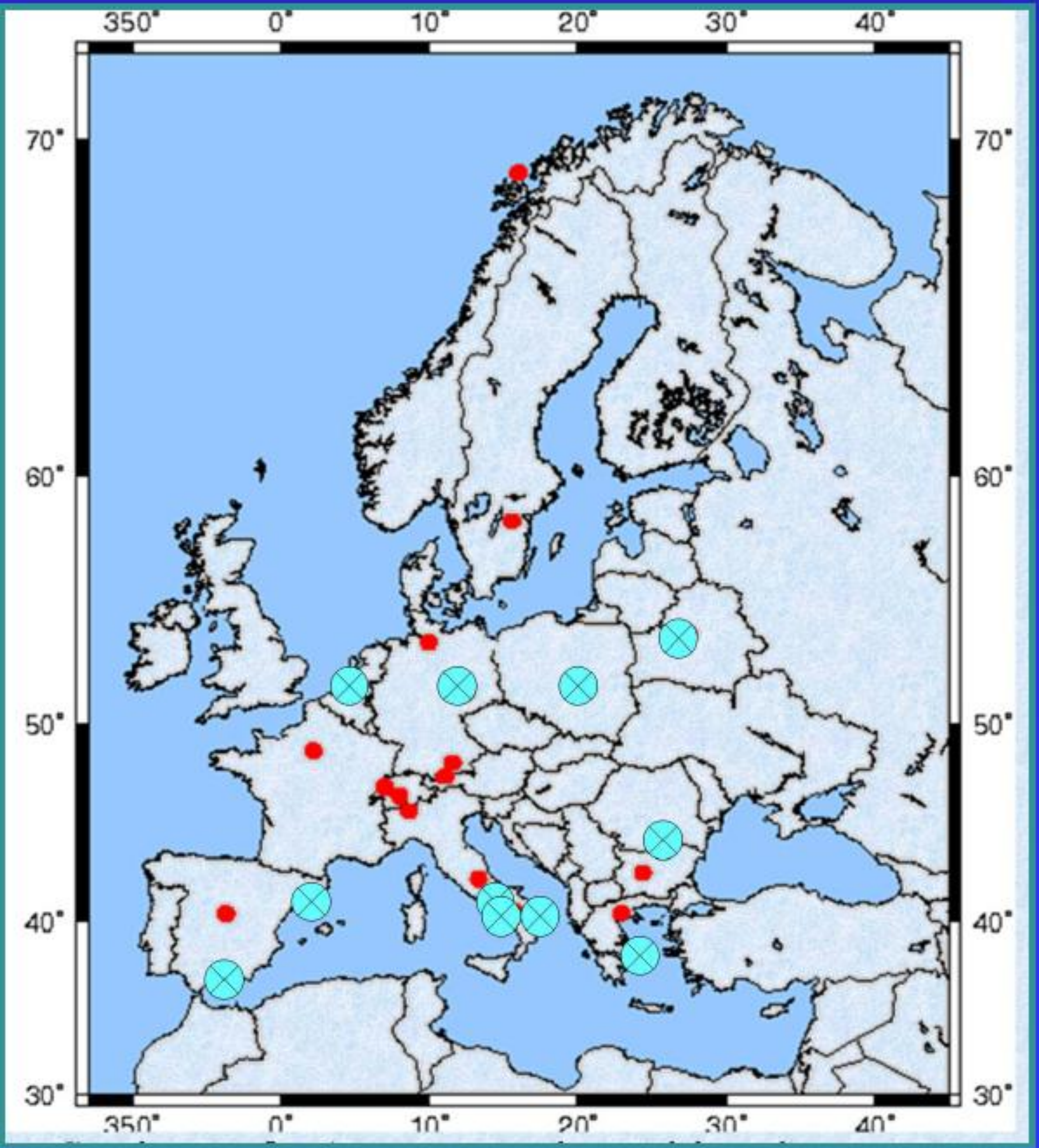

LIRIC is employed !!!

no LIRIC yet …

Slide kindly provided by Oleg Dubovik

Assumptions:

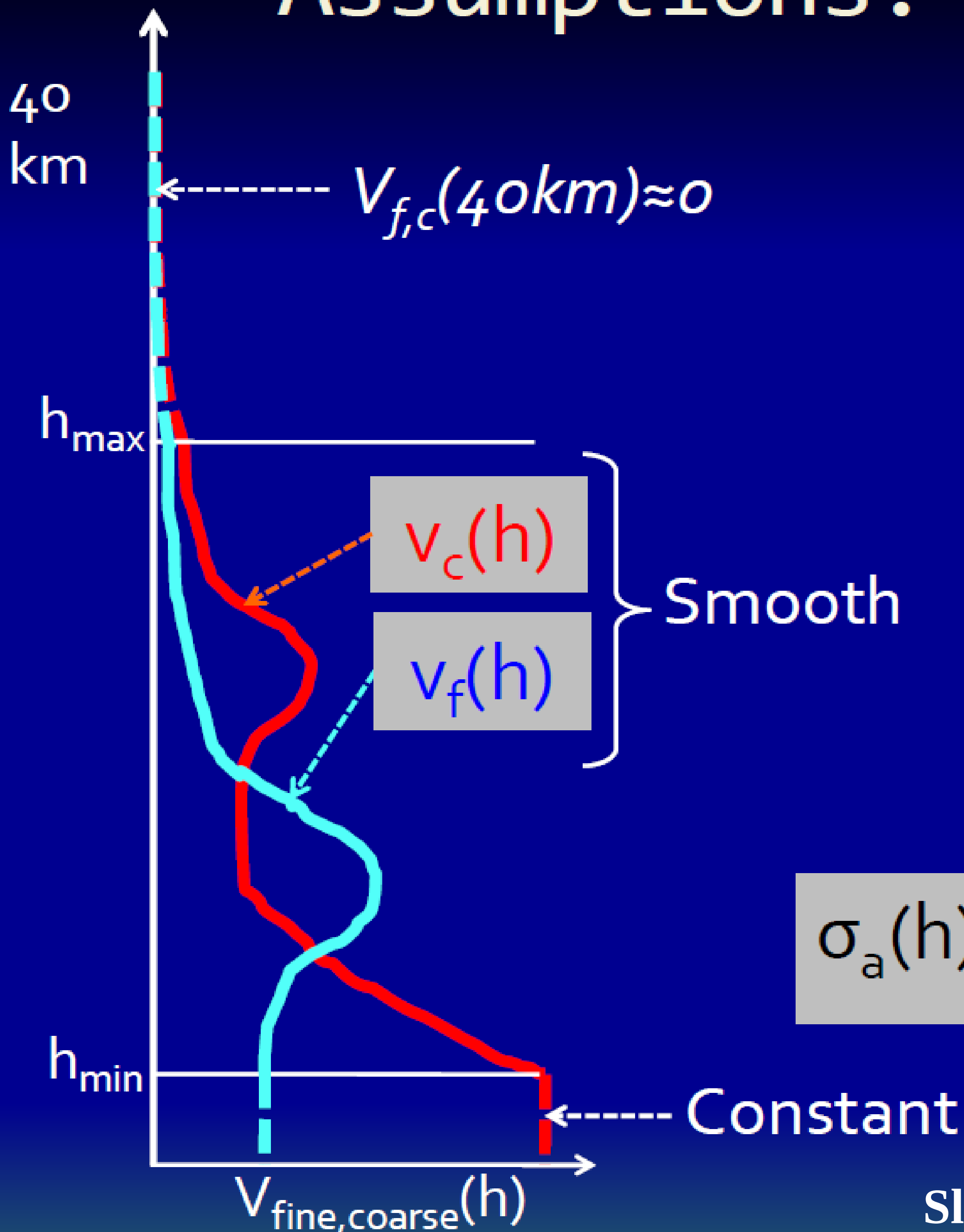

Height independent:

- $dV(r)/d\ln r$,
- $n(\lambda)$, $k(\lambda)$
- $\omega_o(\lambda)$, $P_{ii}(\lambda,\Theta)$

fine & coarse

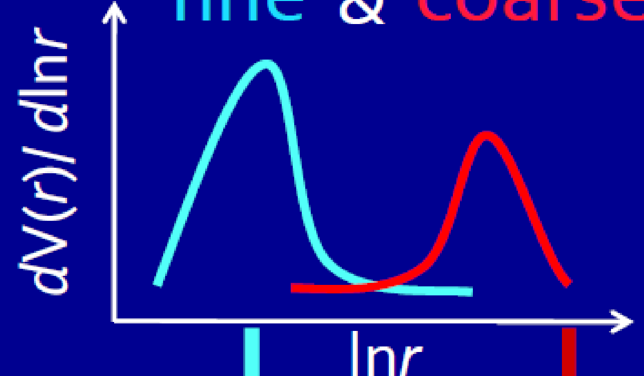

$$\sigma_a(h) = v_f(h)\tau_f^{ext} + v_c(h)\tau_c^{ext}$$

Slide kindly provided by Oleg Dubovik

Limitations of approach

1. Column extinction from Sun photometer is used for calibration, so the lidar profiles should be extrapolated to the ground.
2. Approach may fail if the layers with different parameters exist.
3. Sun photometer measurements are not always available.

We follow the "traditional" approach

Lidar signals → Calculation of α and β → Particle parameters

- **Joint use of α and β - key for successful retrieval.**
- **The most practical configuration of Raman lidar is based on tripled Nd:YAG laser:**
  Three elastic channels and two nitrogen Raman (3+2)
  Backscattering β – 355, 532, 1064 nm
  Extinction α – 355, 532 nm

Two Approaches to Retrieval

Optical data (α or β) at different λ are calculated from equation:

$$g_i = \int_0^\infty K_i\ (m, r, \lambda)\frac{dV(r)}{dr}dr \quad \Rightarrow \quad \mathbf{K}^T\ \mathbf{v} = \mathbf{g}$$

K – discrete kernels
v – discrete volume

Inversion with regularization

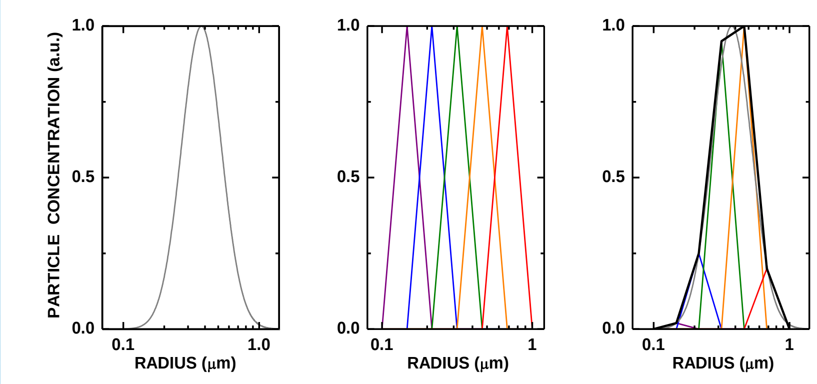

$$\mathbf{v} = \mathbf{B}\mathbf{x}$$

$$\mathbf{g} = \mathbf{K}^{\mathrm{T}}\mathbf{B}\mathbf{x} = \mathbf{A}\mathbf{x}$$

$$\mathbf{x} = \left(\mathbf{A}^{\mathrm{T}}\mathbf{A} + \gamma\mathbf{H}\right)^{-1}\mathbf{A}^T\mathbf{g}$$

Kernels expansion

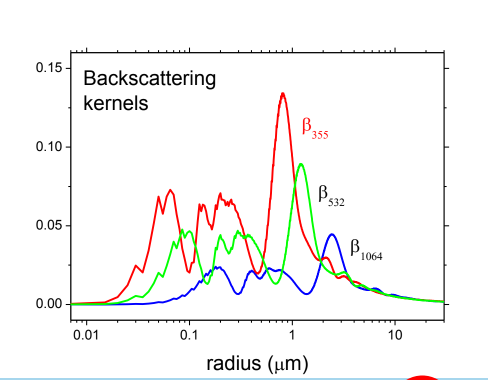

$$\mathbf{v} = \mathbf{K}\mathbf{x} + \mathbf{v}_\perp = \mathbf{v}_g + \mathbf{v}_\perp$$

$$\mathbf{g} = \mathbf{K}^{\mathrm{T}}\mathbf{K}\ \mathrm{x} + \mathbf{K}\ \mathbf{v}_\perp = \mathbf{K}^{\mathrm{T}}\mathbf{K}\ \mathrm{x}$$

$$\mathbf{x} = \left(\mathbf{K}\mathbf{K}^{\mathrm{T}}\right)^{-1}\mathbf{g}$$

The problem is underdetermined!

We make a set of initial guesses about:

- Real and imaginary parts of CRI m_R, m_I
- Maximal and minimal particle radii r_{max}, r_{min} (inversion interval)

Instead a single solution we have a family of solutions.

Solutions are selected on a base of discrepancy.

Two ways to calculate the discrepancy

Inversion with regularization

Optical data g

↓ assume m, r_{min}, r_{max}

Solution f_i

↓ $\mathbf{g}^{\delta} = \hat{\mathbf{A}} | f_i |$

Back-calculated g^{δ}

↓

$\mathbf{g} - \mathbf{g}^{\delta}$

Discrepancy is minimized by adjusting Lagrange multiplier, so it controls the smoothness of solution

Kernels expansion

One optical data g_i is estimated from the rest of N-1 measurements

N-1 data

↓ assume m, r_{min}, r_{max}

$\mathbf{g}_i^{\delta}$

↓

$\mathbf{g}_i - \mathbf{g}_i^{\delta}$

Discrepancy describes the consistency of optical data for the found solution

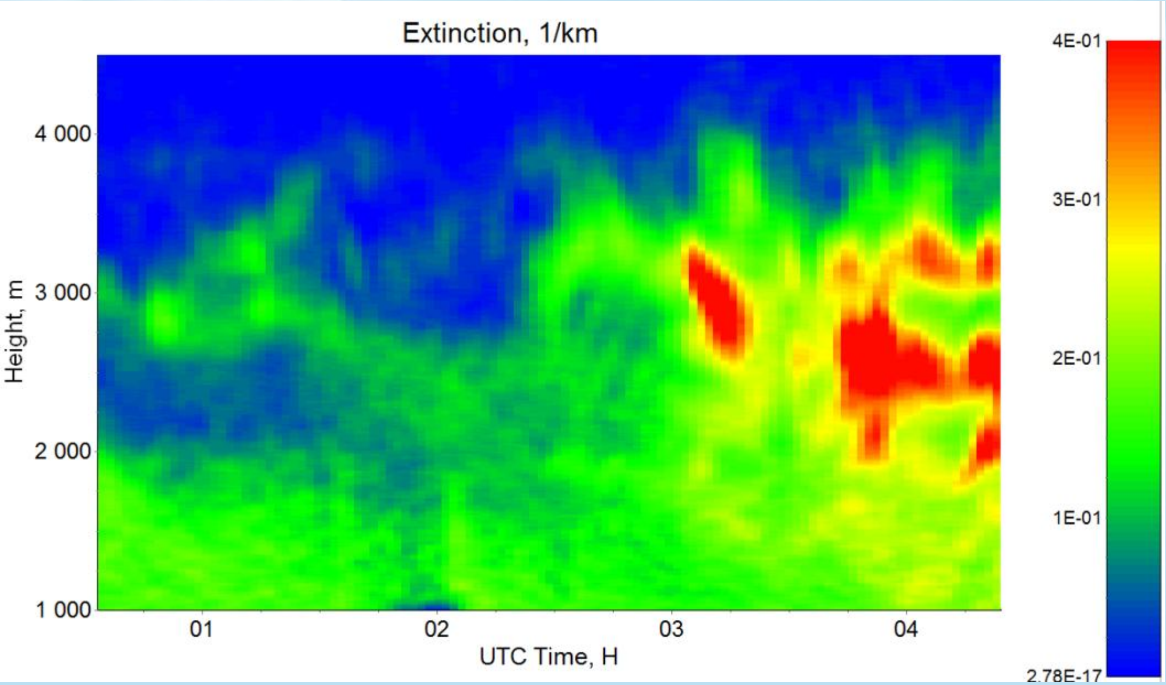

Example of “data quality control” via discrepancy

Extinction at 355 nm calculated by Raman

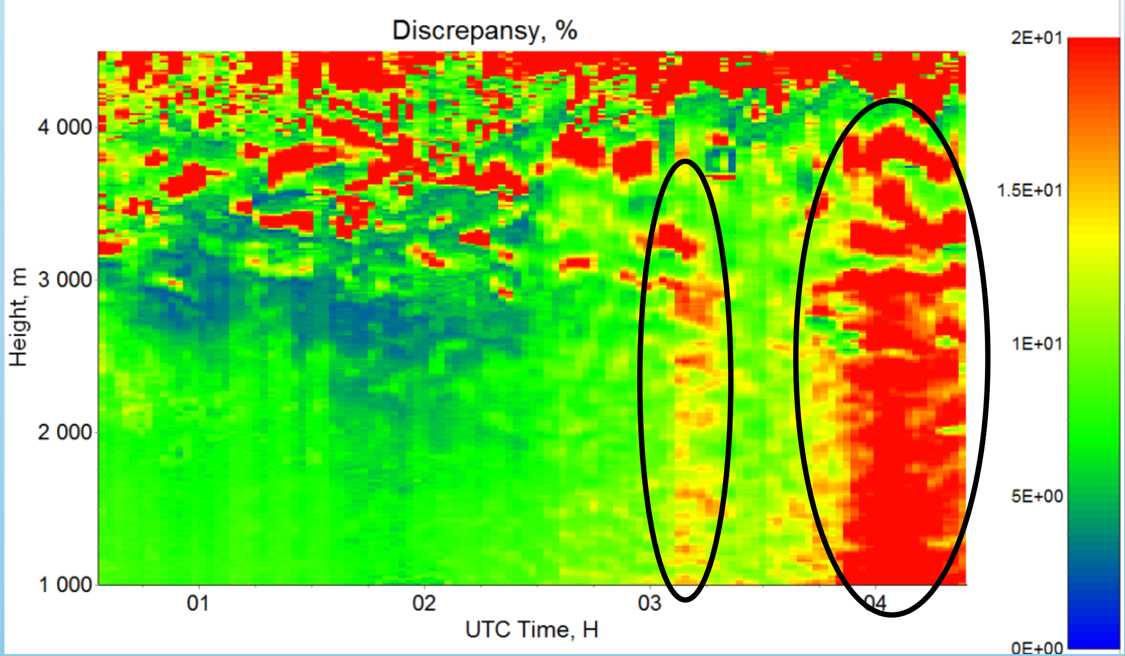

Discrepancy of 3+1 data In the areas marked with red the data are inconsistent

Estimation of complex refractive index

“Dream” case

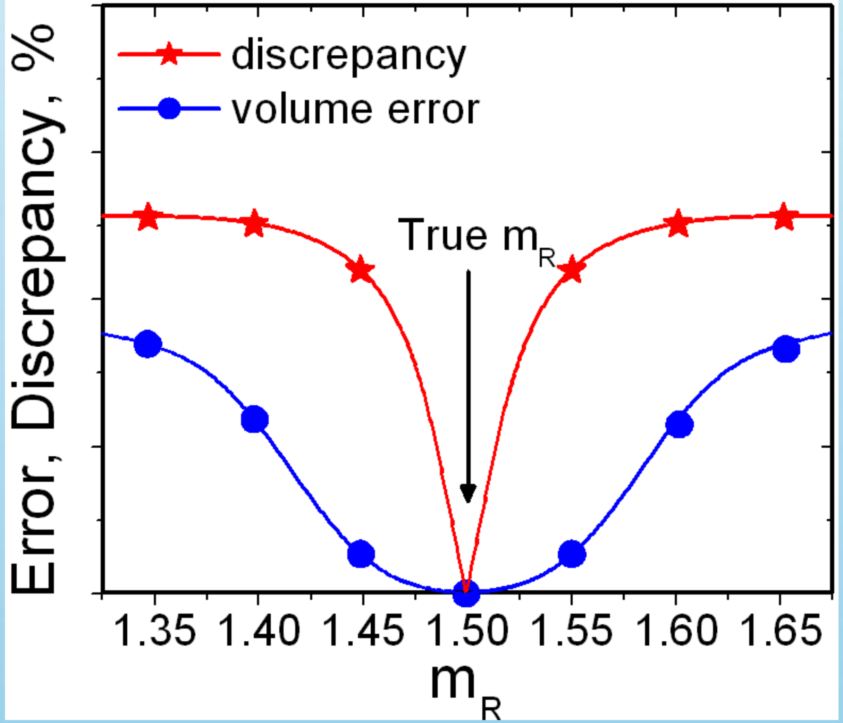

“Nightmare” case

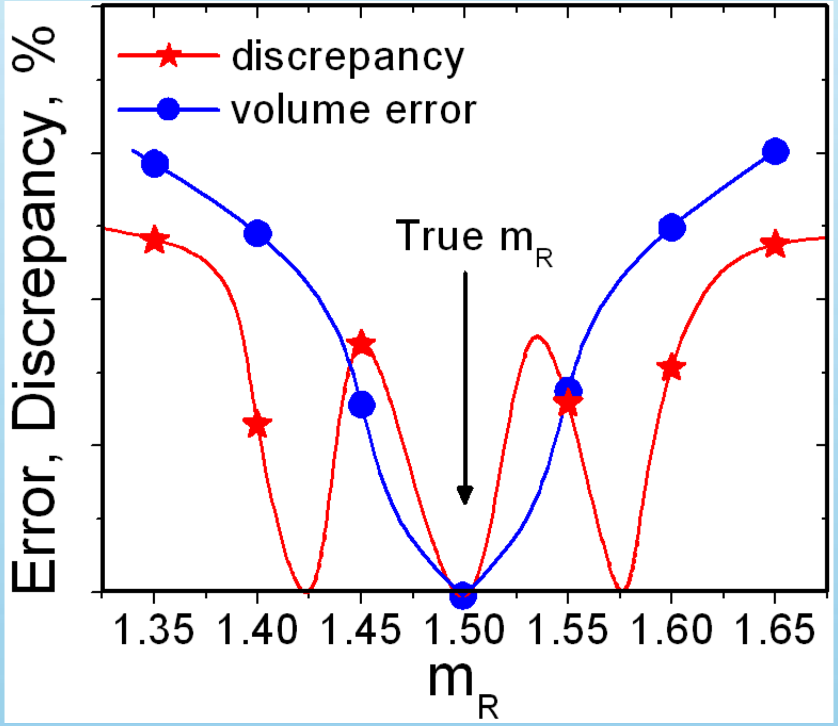

Modeling of realistic case

Inversion with regularization

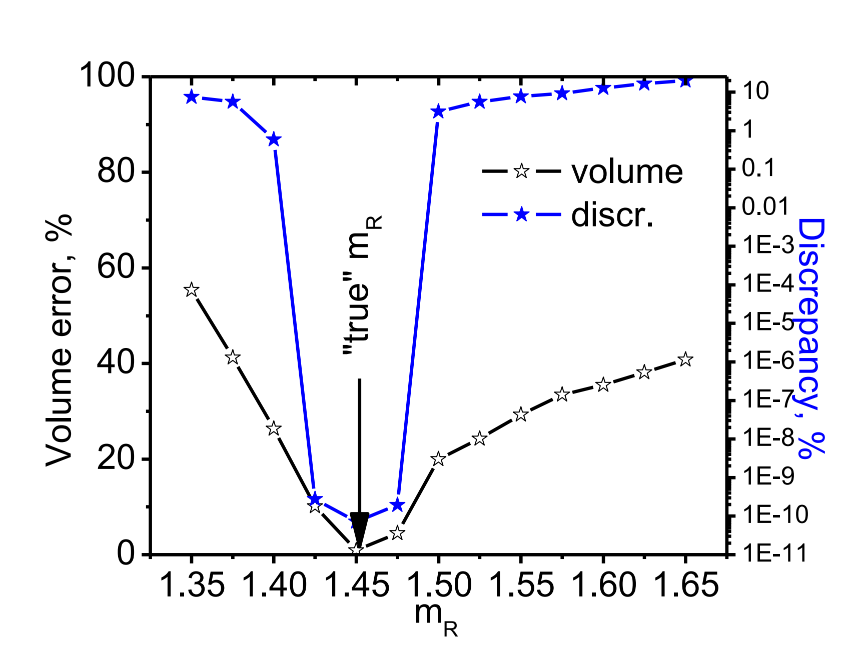

Kernels expansion

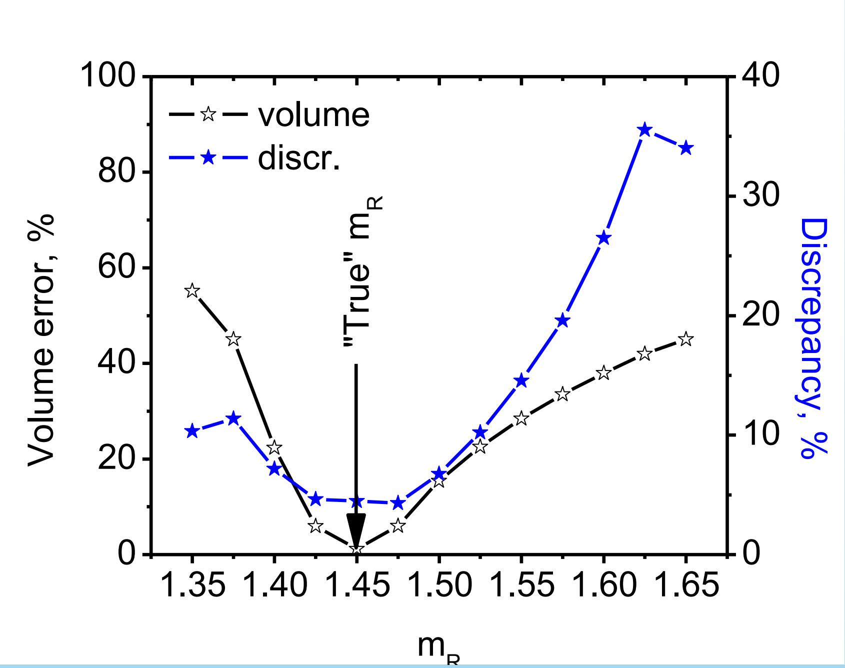

Simulation was performed for the fine mode particles

Result depends on the range of imaginary part variation

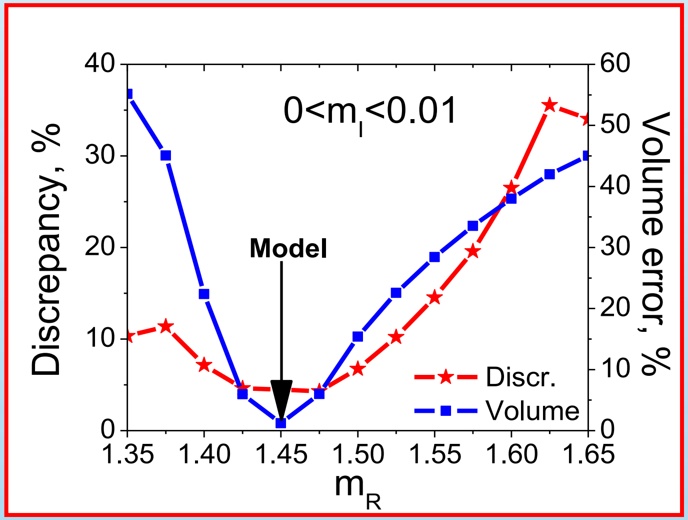

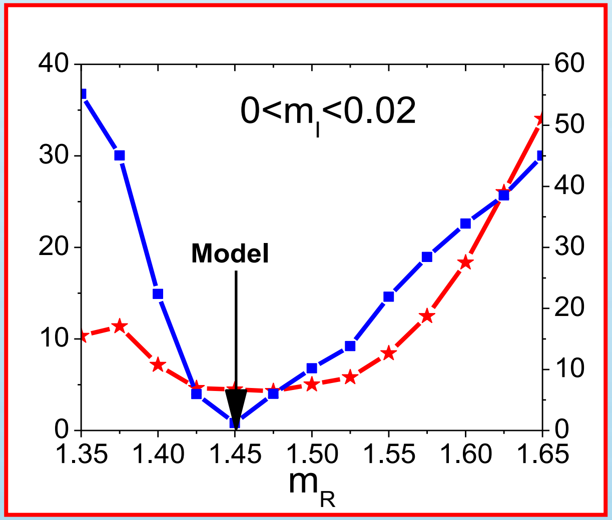

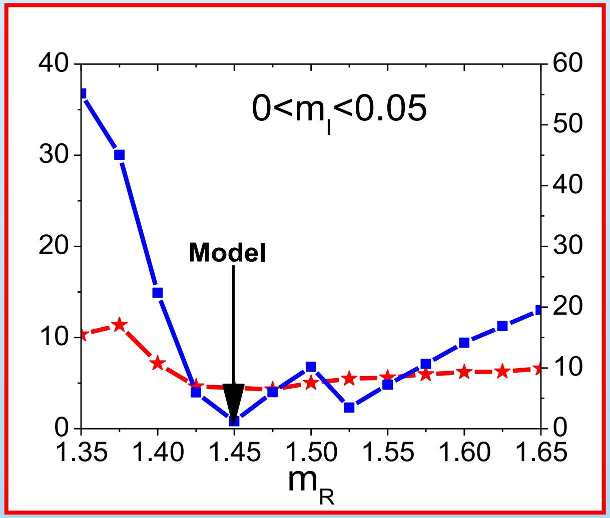

Example of simulation for the fine mode of PSD. Different ranges of m_I variation are considered.

Model value of CRI is m=1.45-i0.005

Comparison of regularization and linear estimation techniques

Optical data

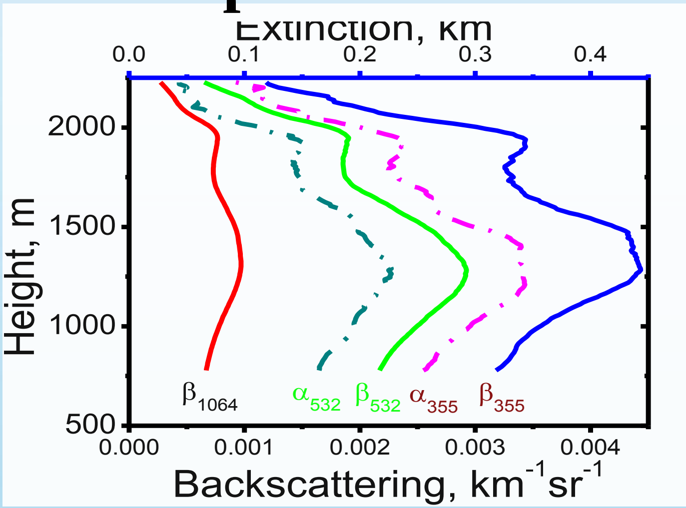

Volume

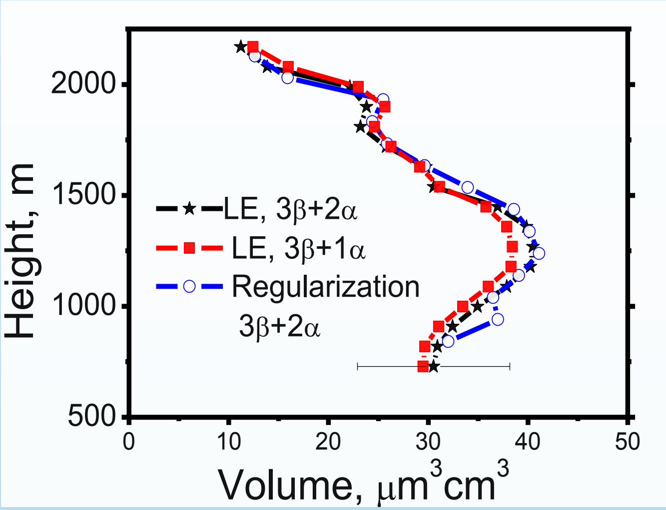

Eff. radius

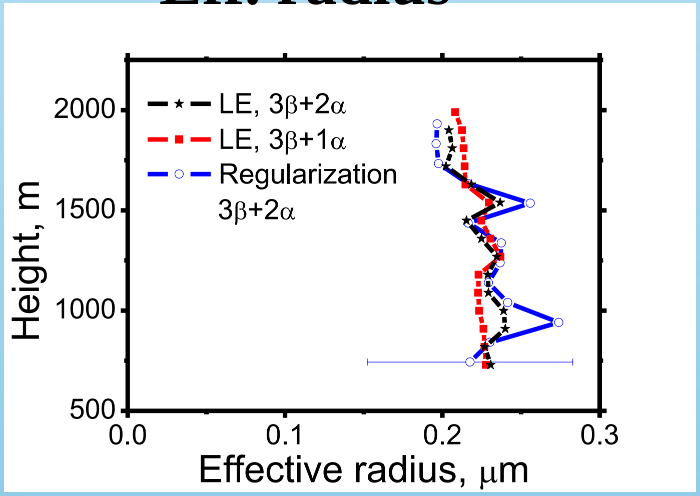

Real part

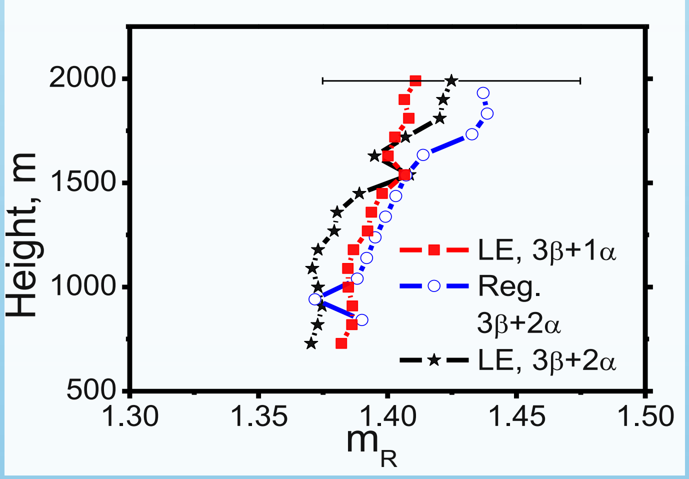

DISCOVER-AQ 2011 CAMPAIGN

The P-3B aircraft carried a suite of nine scientific instruments including NASA LARC HSRL system.

14 flights occurred during June 27 - July 31 period over Baltimore – Washington area.

GSFC multiwavelength Raman lidar performed the measurements from the ground

Lidar parameters:
Telescope aperture 400 mm
Laser power at 355 nm – 20 W

Operational wavelengths:
elastic – 355, 532, 1064 nm
Raman – 387, 608, 408 nm

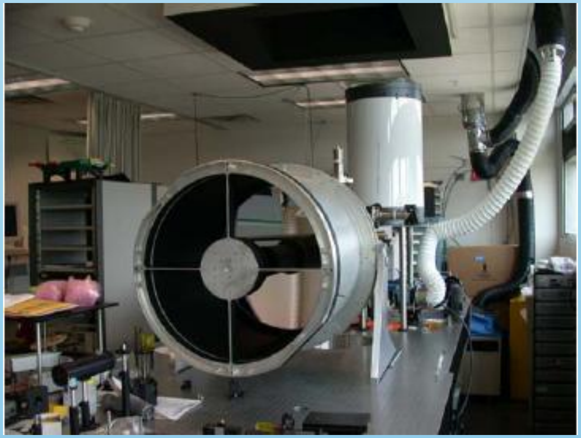

- Temporal resolution of the measurements – 2 min.
- Measurements are vertical, height resolution 15 m.
- Sonde data are from Beltsville (~5 miles apart)

20 – 21 July measurements

Extinction at 355 nm by Klett

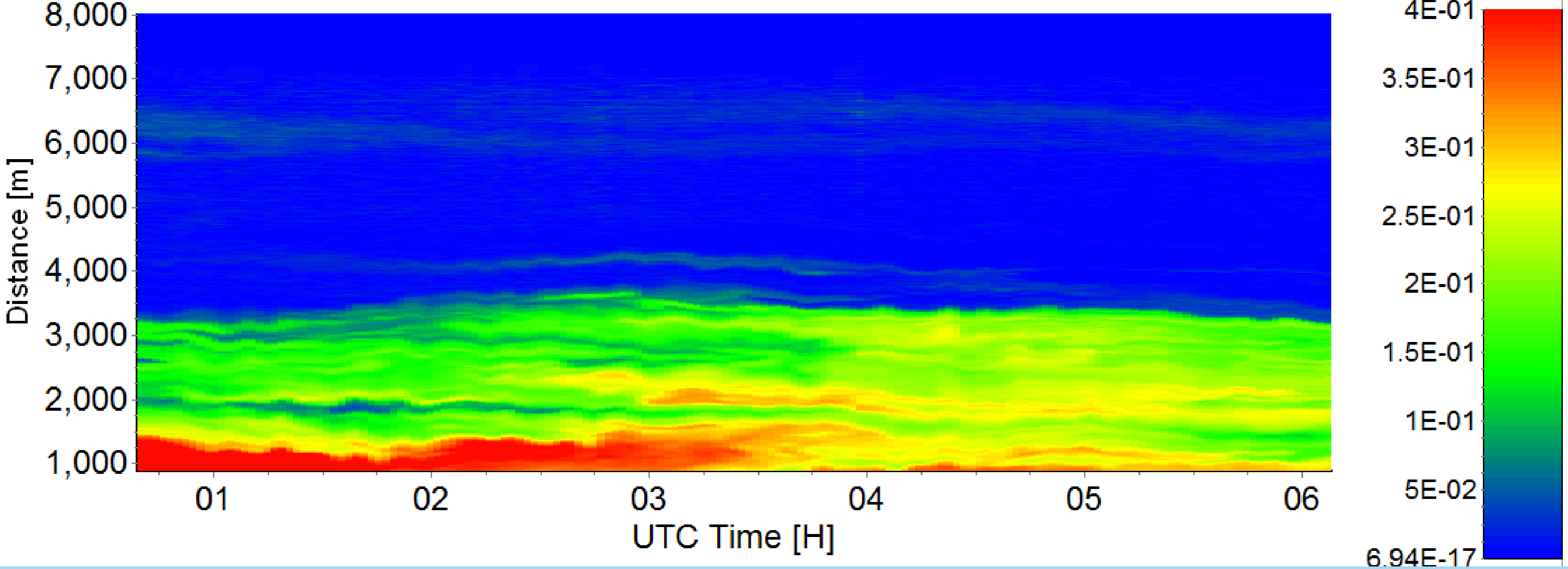

Aerosol is represented mainly by sulfates and biomass burning products. RH is insufficient for significant hygroscopic growth.

Retrieval of height – temporal distributions of particle parameters

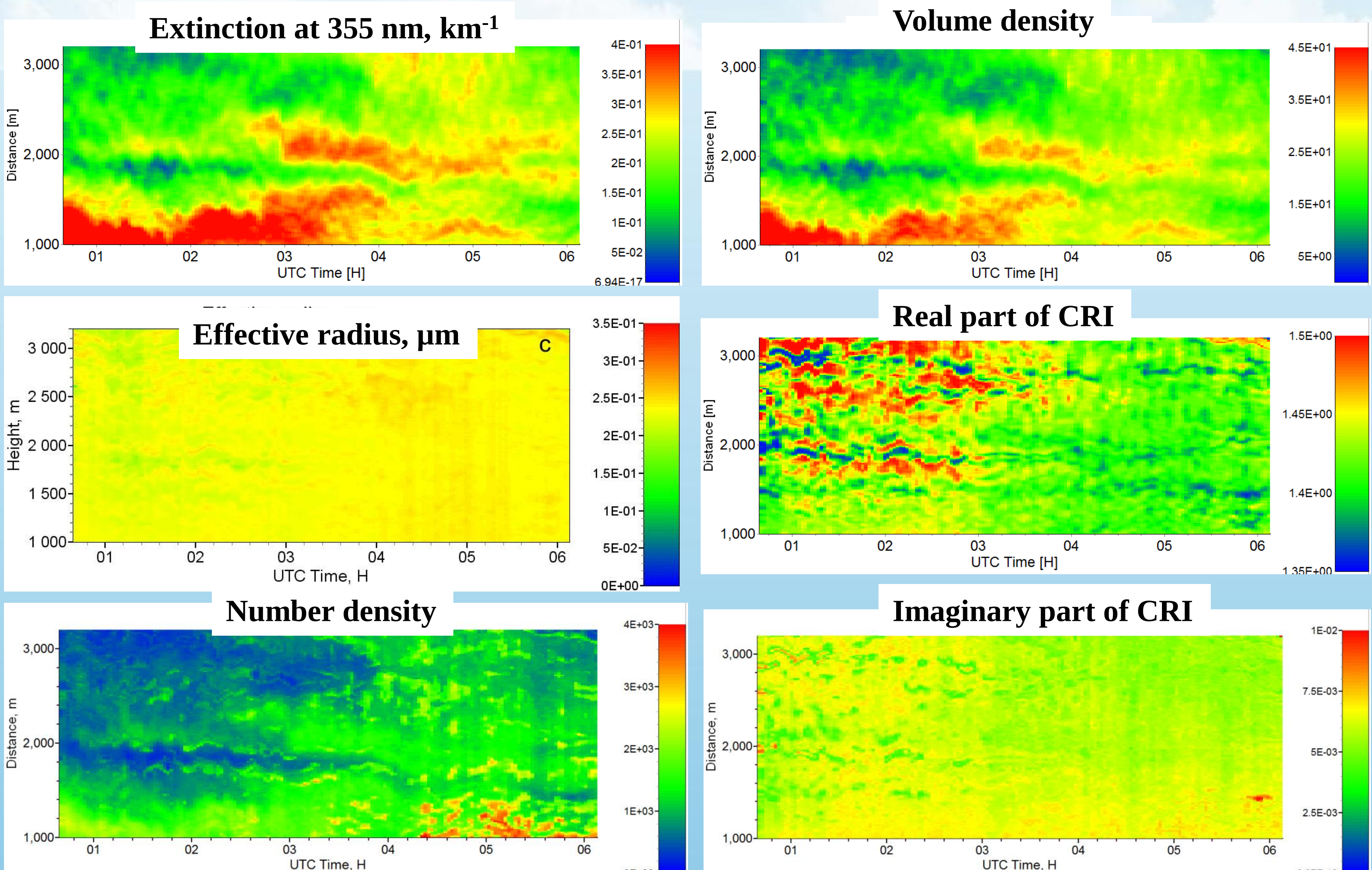

Comparison with AERONET

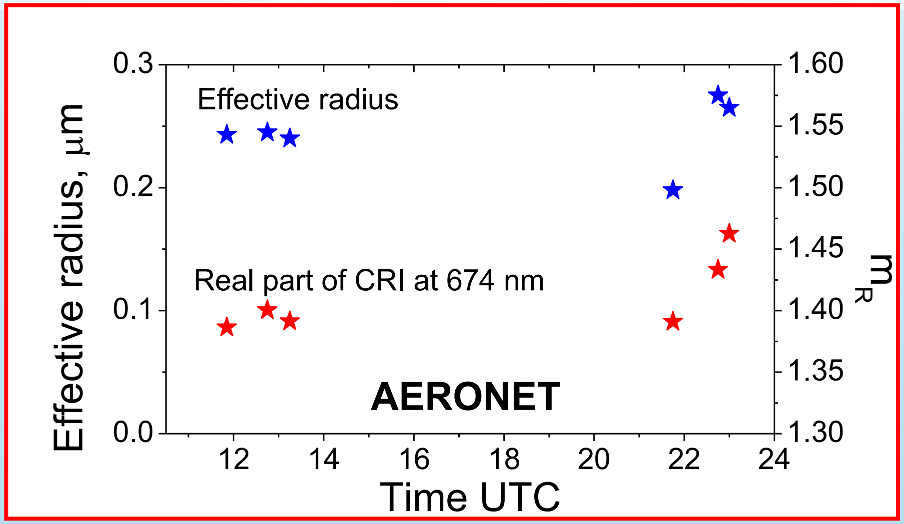

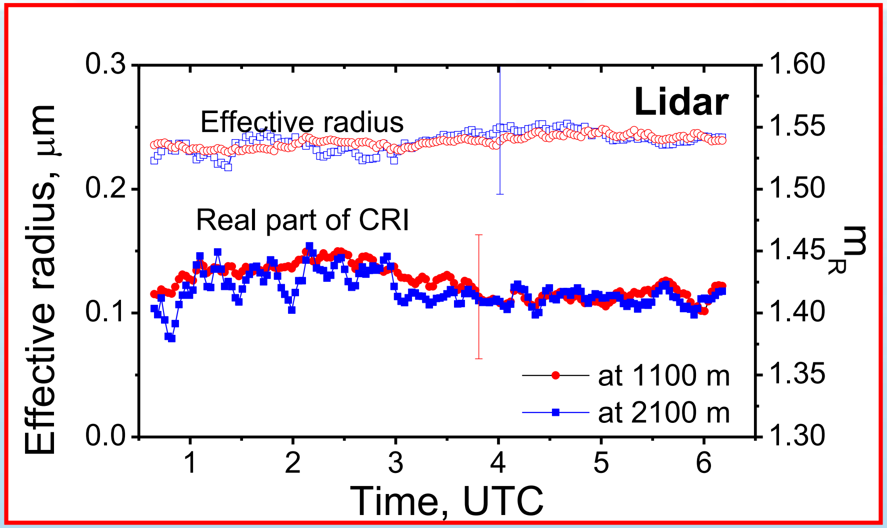

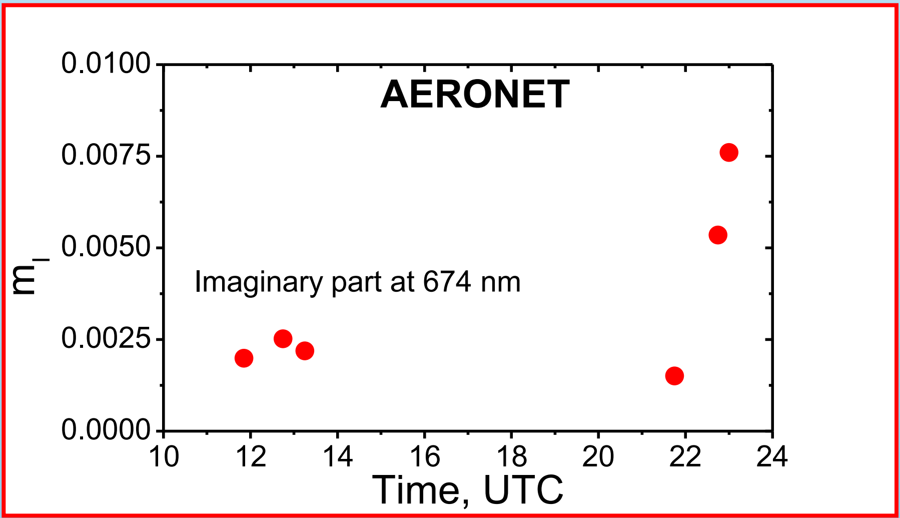

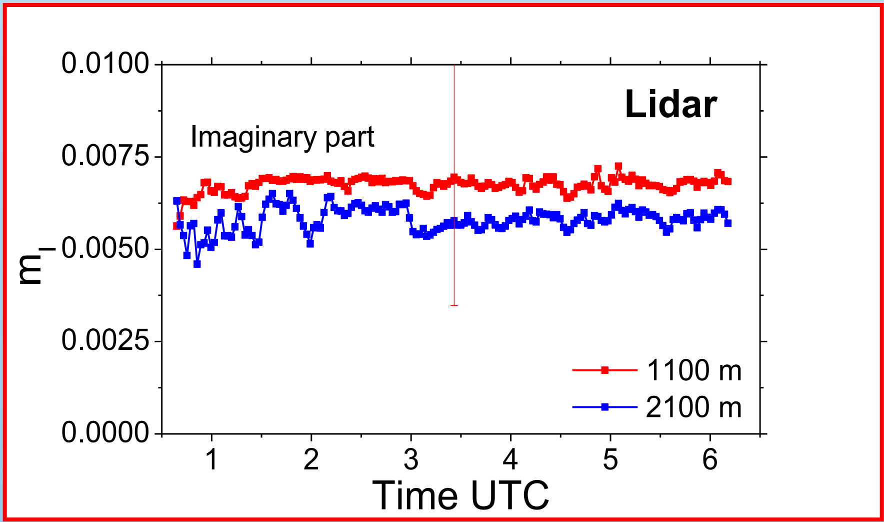

Lidar derived column volume

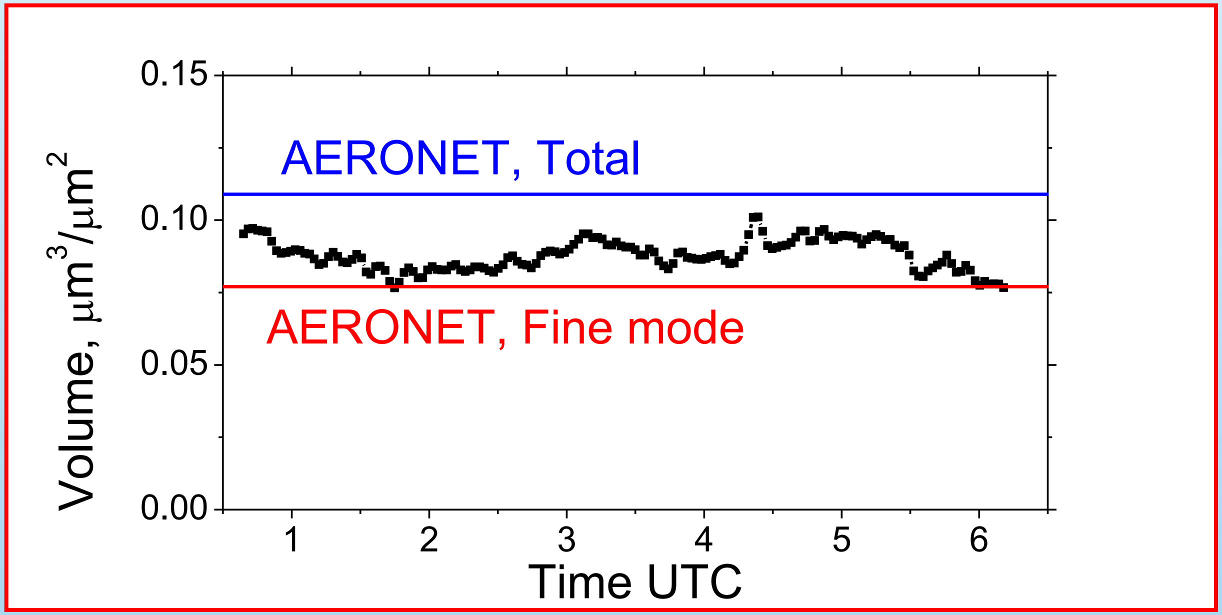

Volume profiles are extrapolated as constant below 1000 m.
For comparison AERONET results at 23:00 UTC are shown.

21 – 22 July measurements

Extinction at 355 nm by Klett

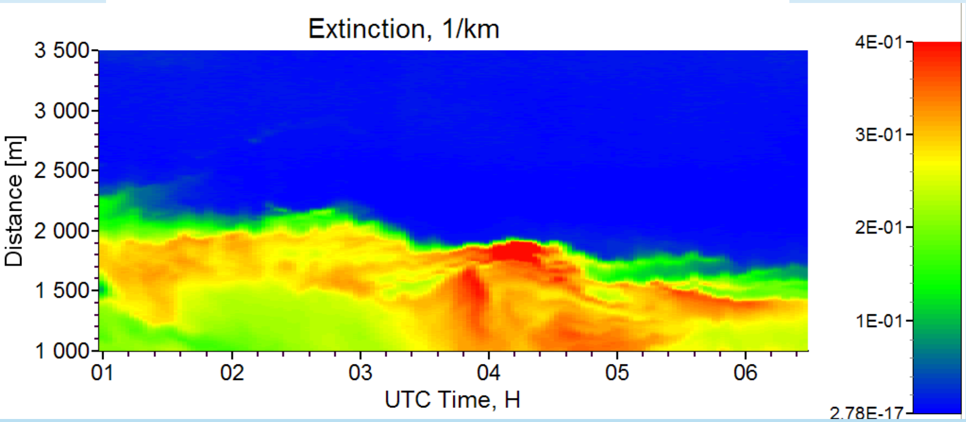

RH from sonde

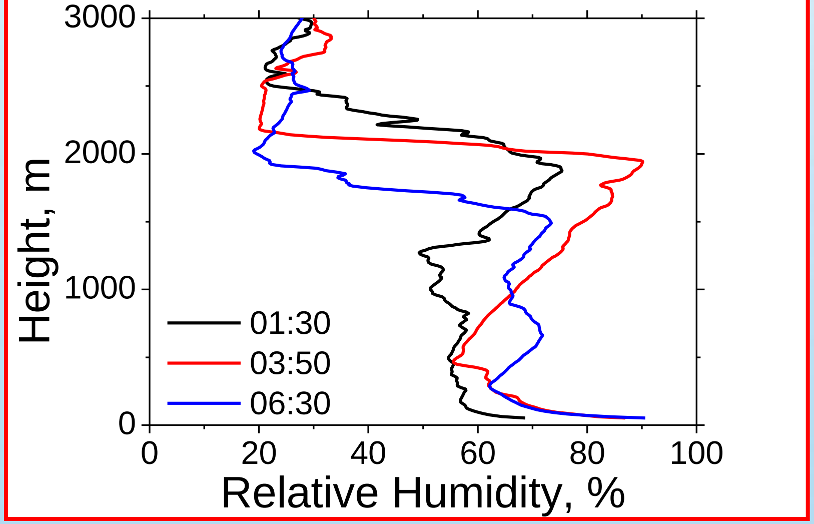

At 03:50 RH is increased up to 90% near the PBL top

Lidar ratio at 355 nm

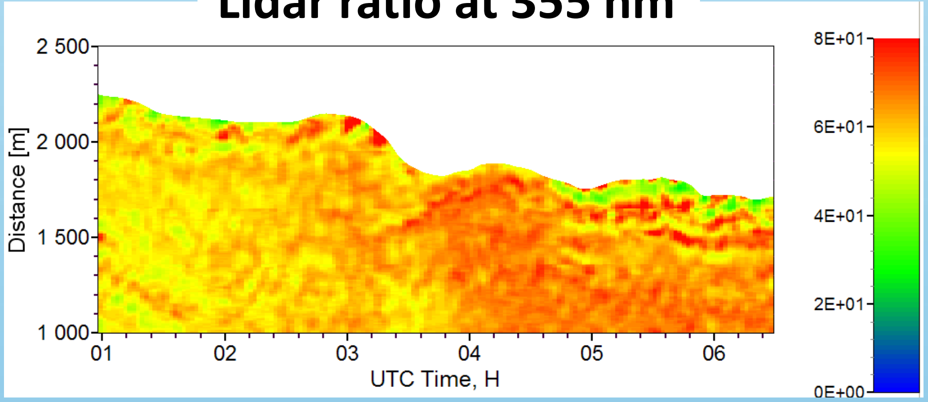

Discrepancy

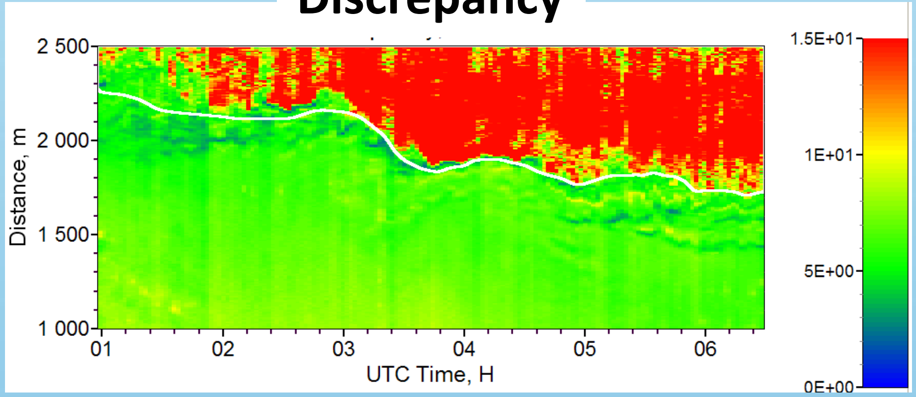

Extinction at 355 nm, km^{-1}

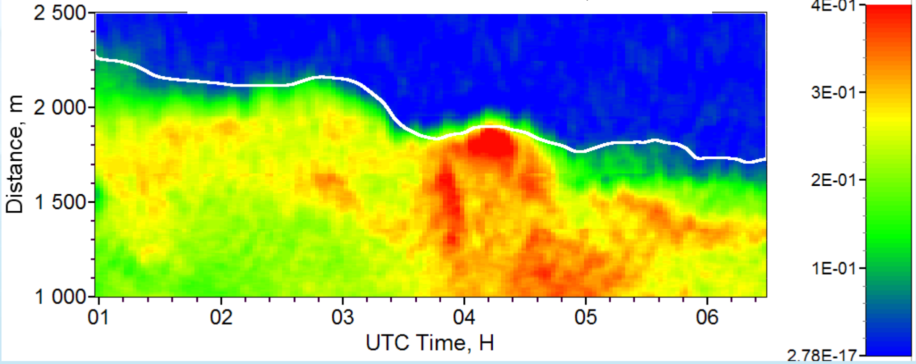

Effective radius

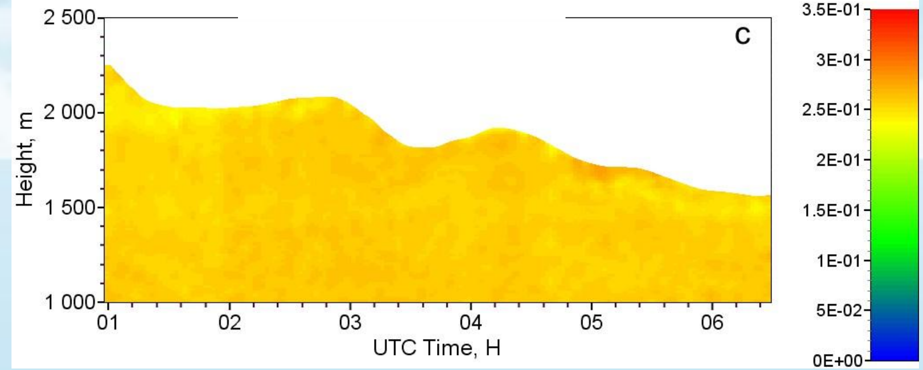

Volume, $\mu m^3/cm^3$

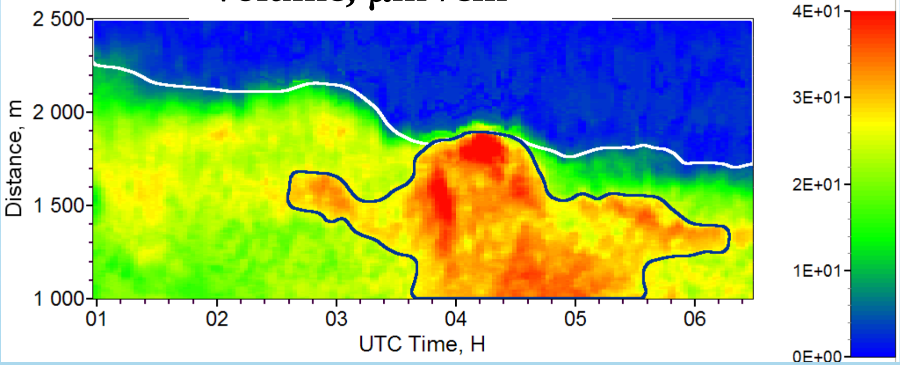

Real part of CRI

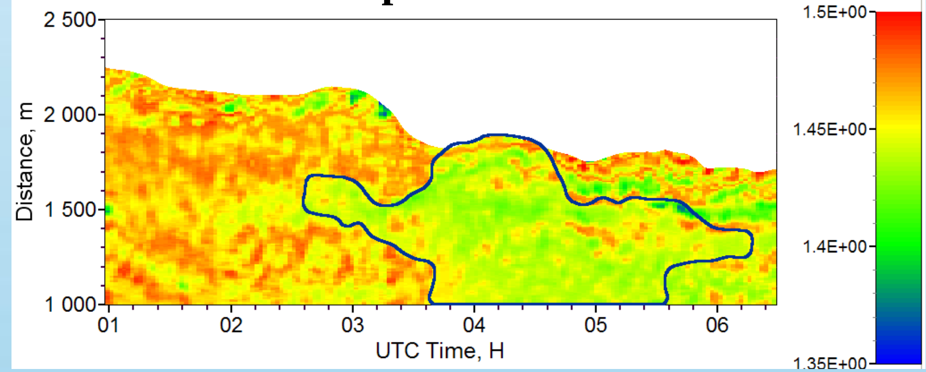

Water vapor mixing ratio

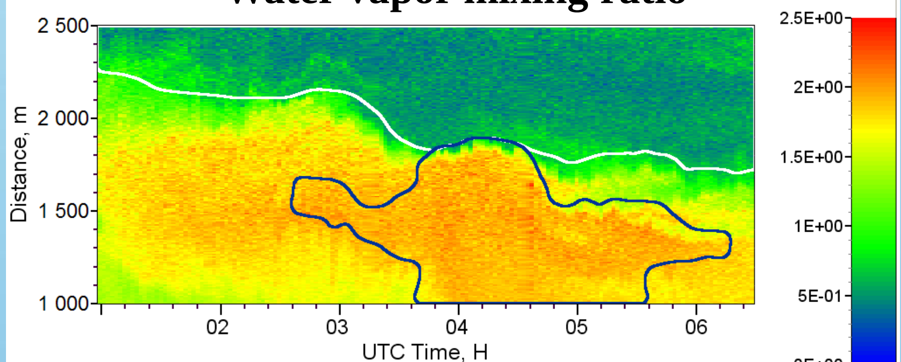

Imaginary part of CRI

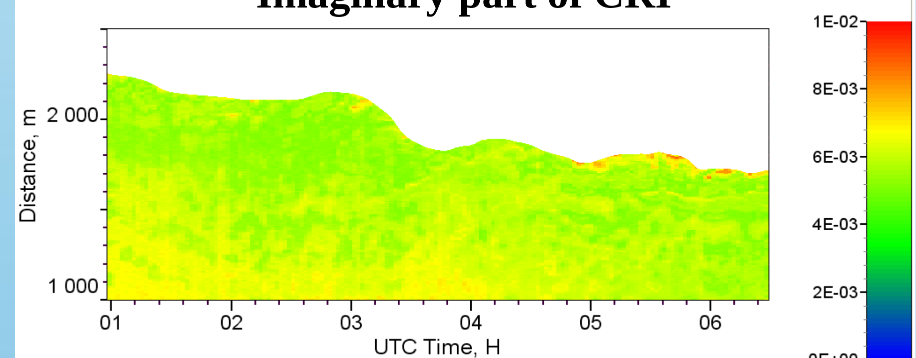

Comparison with AERONET

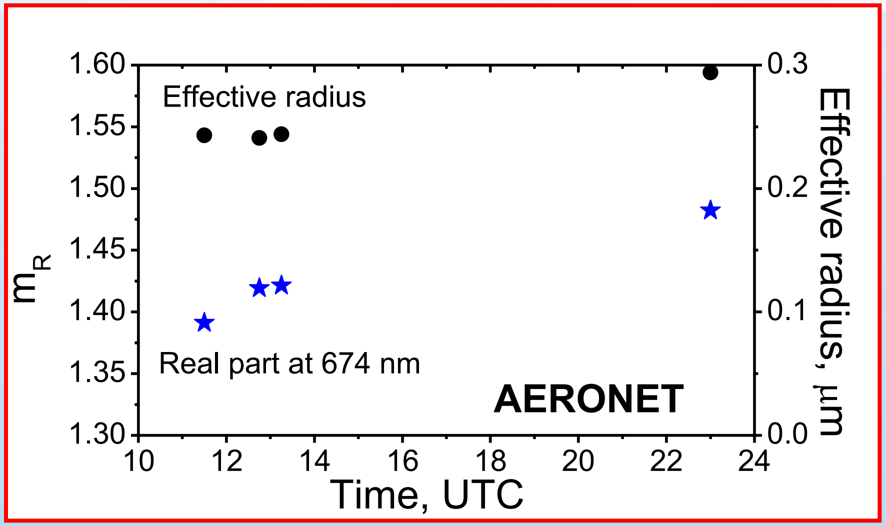

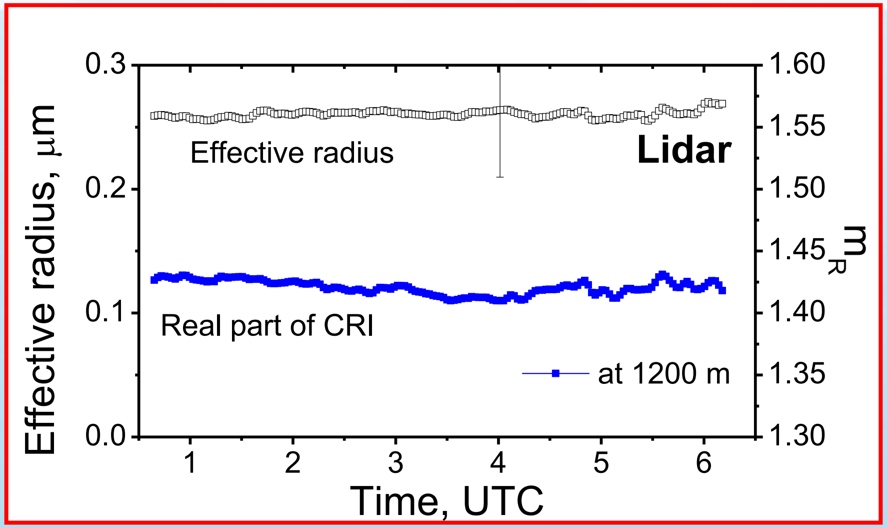

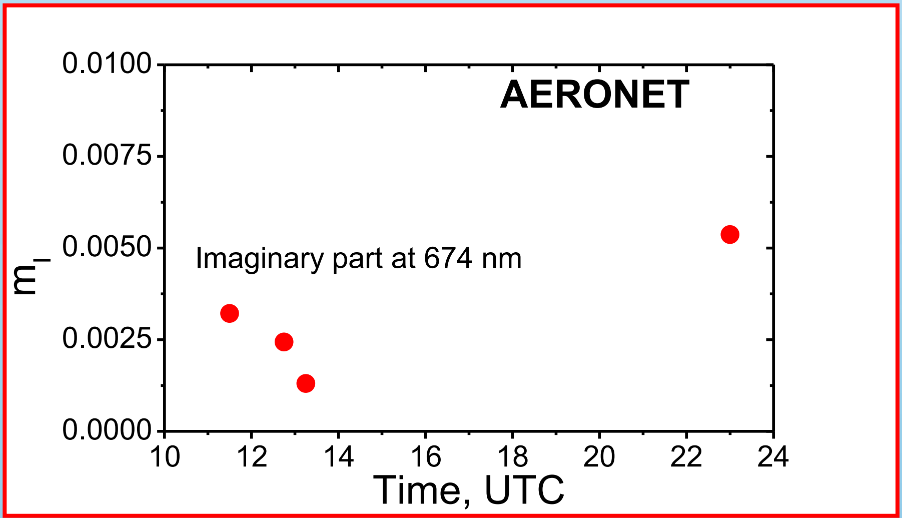

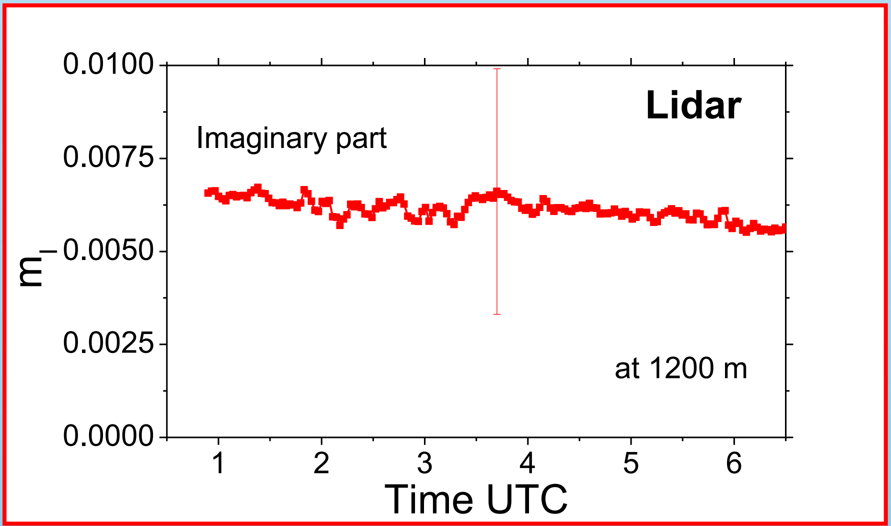

Treatment of Dust Particles

from M.Wiegner et al.

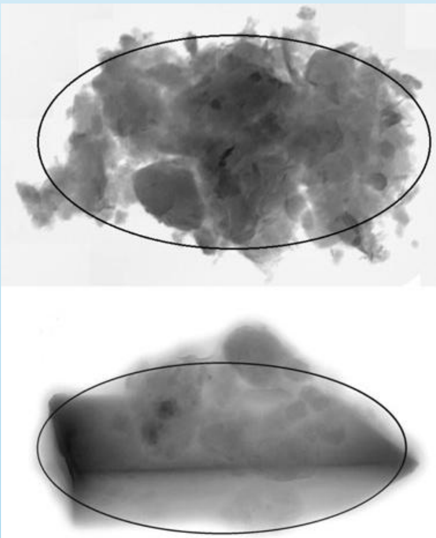

Main Idea: generalizing aerosol modeling by using randomly oriented spheroids instead of spheres (*Mishchenko et al. 1997)*

Parameters: $dV(r)/d\ln r$, + $dn(\varepsilon)/d\ln\varepsilon$

r - radius of volume-equivalent sphere

ε - aspect ratio

The positive experience of AERONET is used:

- Aerosol is mixture of spheres and spheroids

$$\frac{\partial V(r)}{\partial \ln r} = \frac{\partial V^{s}(r)}{\partial \ln r} + \frac{\partial V^{un}(r)}{\partial \ln r}$$

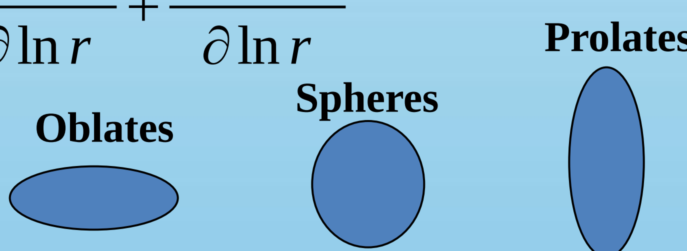

from O.Dubovik

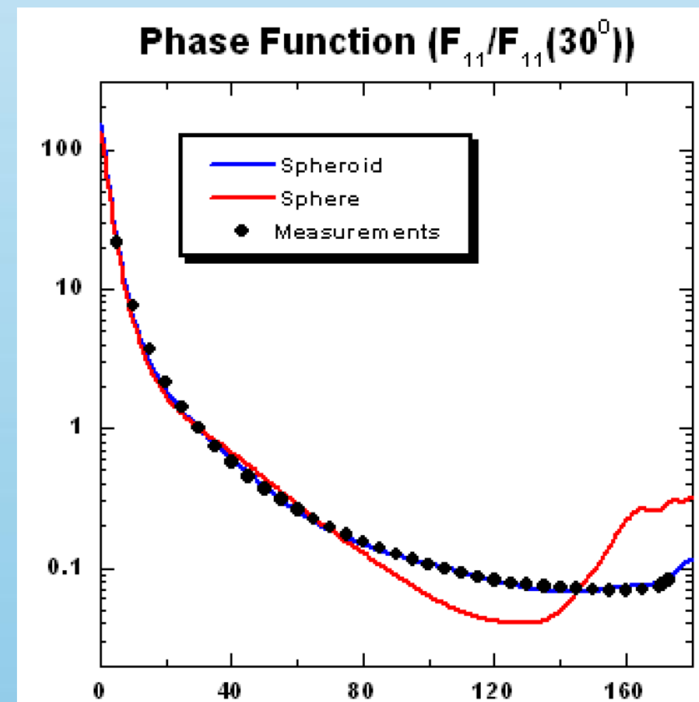

Spheroidal model is simplified

- Aspect ratio distribution of spheroids is size independent;
- Aspect ratio distribution of spheroids is fixed (to match laboratory measured phase function);
- Prolates or oblates contribute equally;

Only one additional parameter appears comparing with spherical particles: spheroids volume fraction η

$$\mathbf{g} = \mathbf{A}(\eta, m)\ \mathbf{C}$$

$$A_{pj}(\eta, m) = \int_{r_{\min}}^{r_{\max}} [(1-\eta) K_p^s(m,r) + \eta K_p^{un}(m,r)] B_j(r) dr$$

Difference between spheres and spheroids

Scattering for spheres (s) and spheroids (ns)

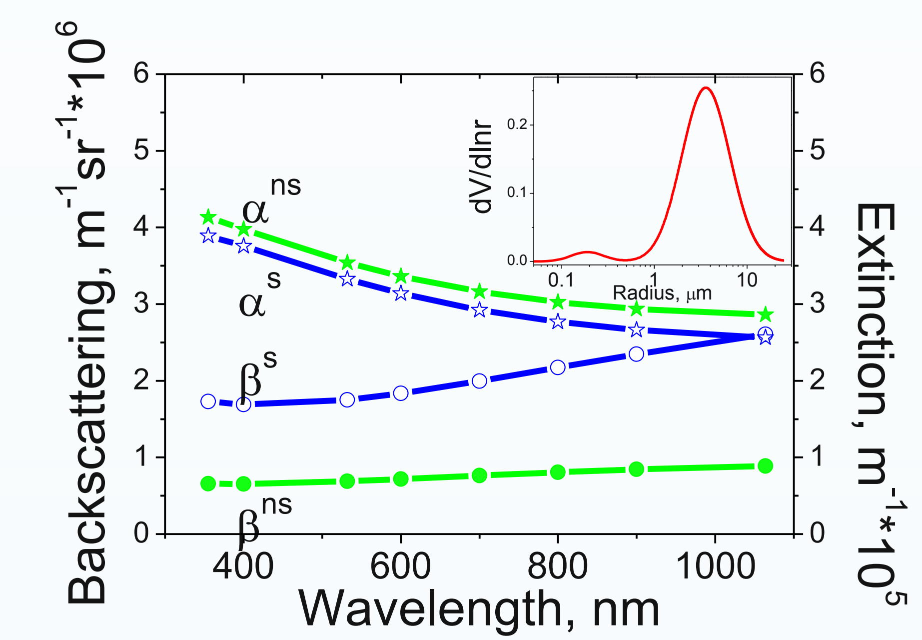

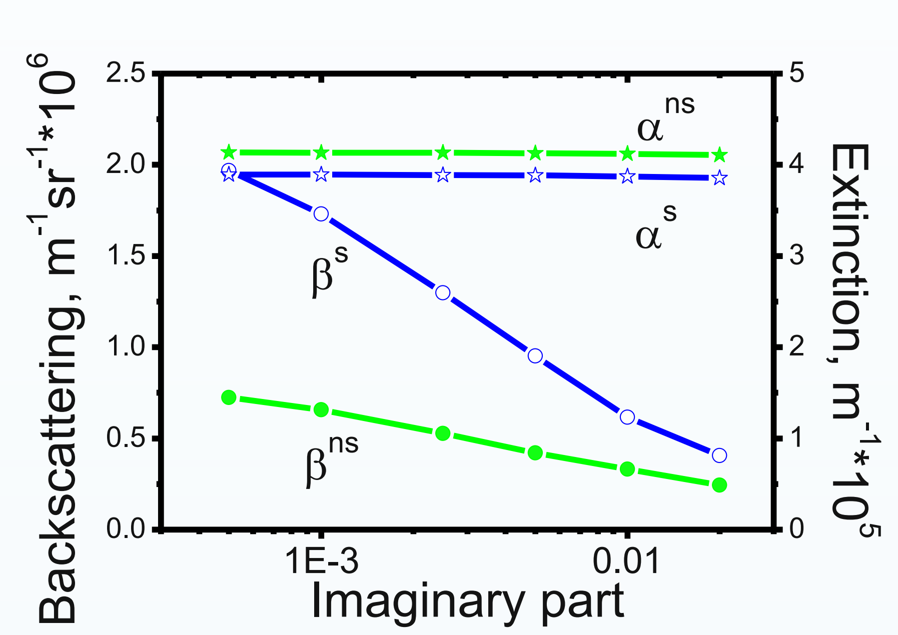

Can we use depolarization in retrieval?

From Dubovik et al

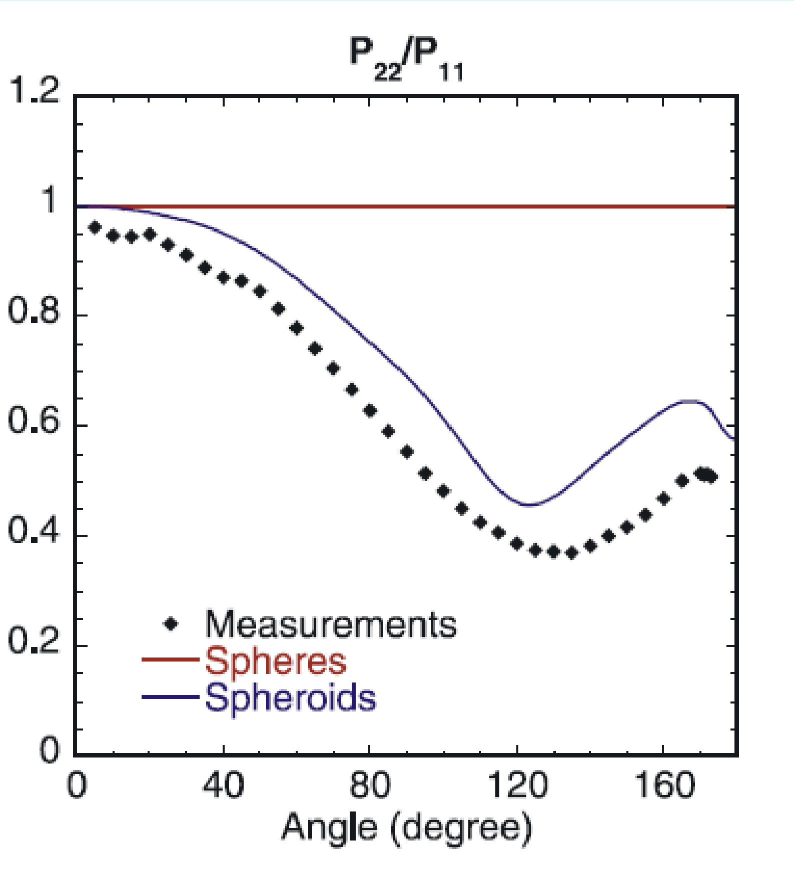

Experimental data of Volten

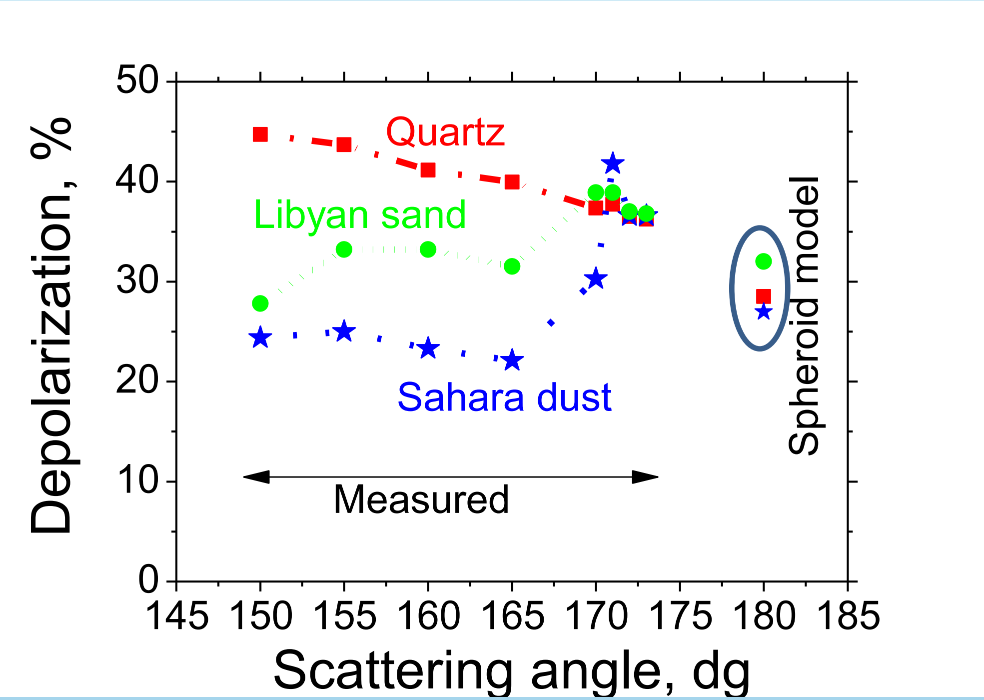

How many depolarizations do we need?
One…

Predictions of spheroid model for depolarization

Depolarization vs particle radius

From O.Dubovik et al.

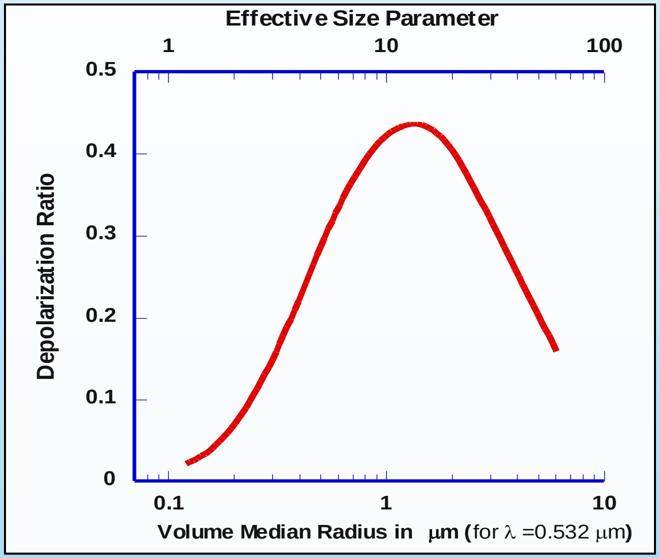

From Gasteiger et al, Tellus 2011

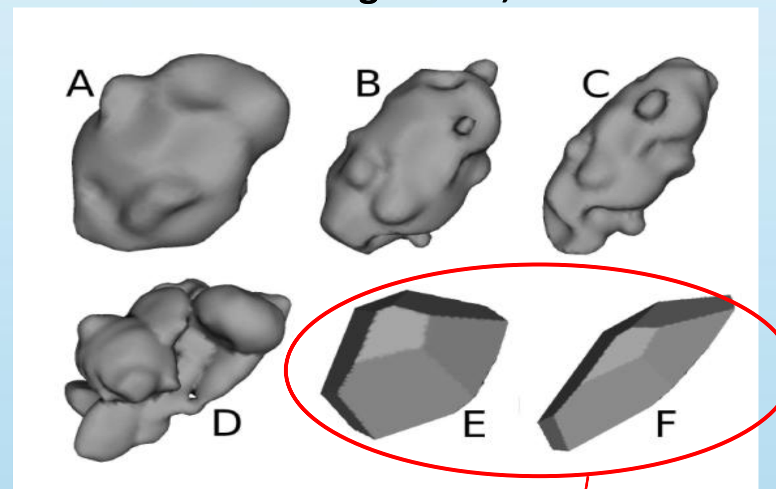

Depolarization vs imaginary part

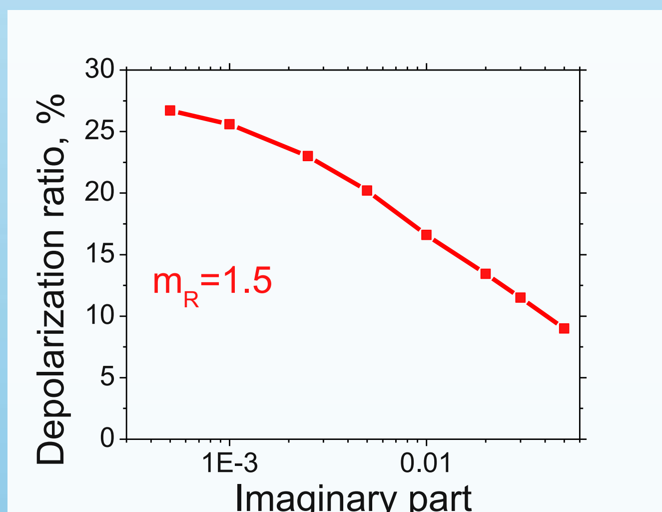

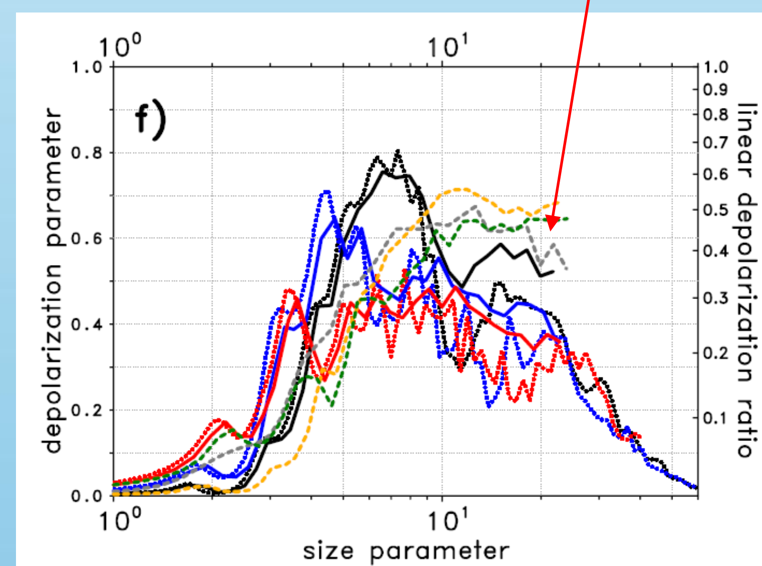

Saharan dust outbreak, Achern 2007

Data of Paolo Di Girolamo

Time evolution of the particle backscatter ratio at 1064 nm. Dust outbreak occurs on 1 August 2007 around 18:00. In the centre of plume the coarse mode dominates PSD.

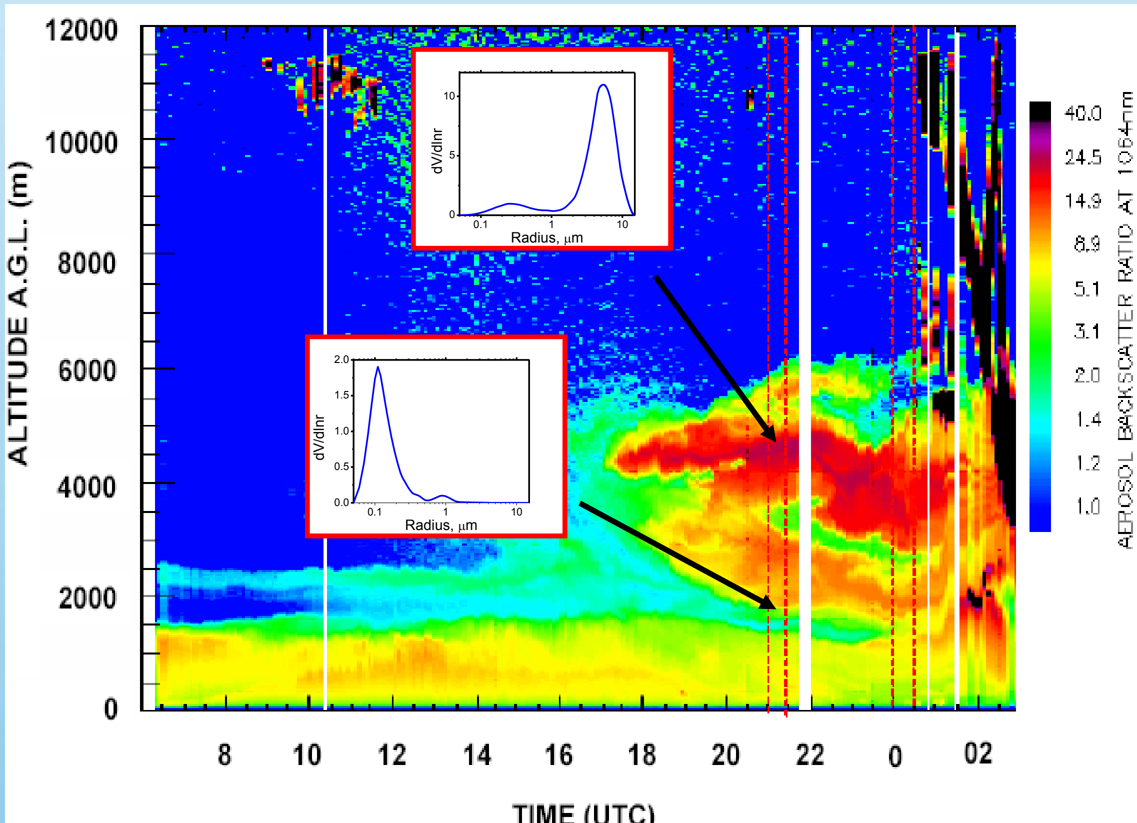

Back trajectories

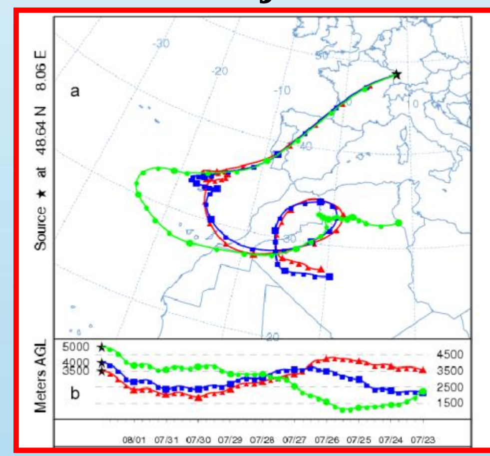

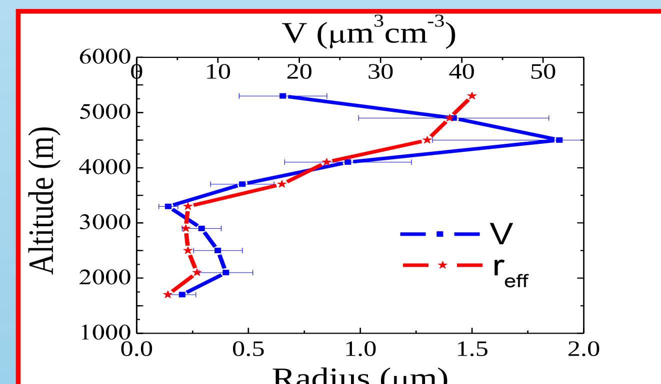

Profile of volume density and effective radius

Application of algorithm to experimental data of M.Tesche et al. from SAMUM-1 (May 19, 2006)

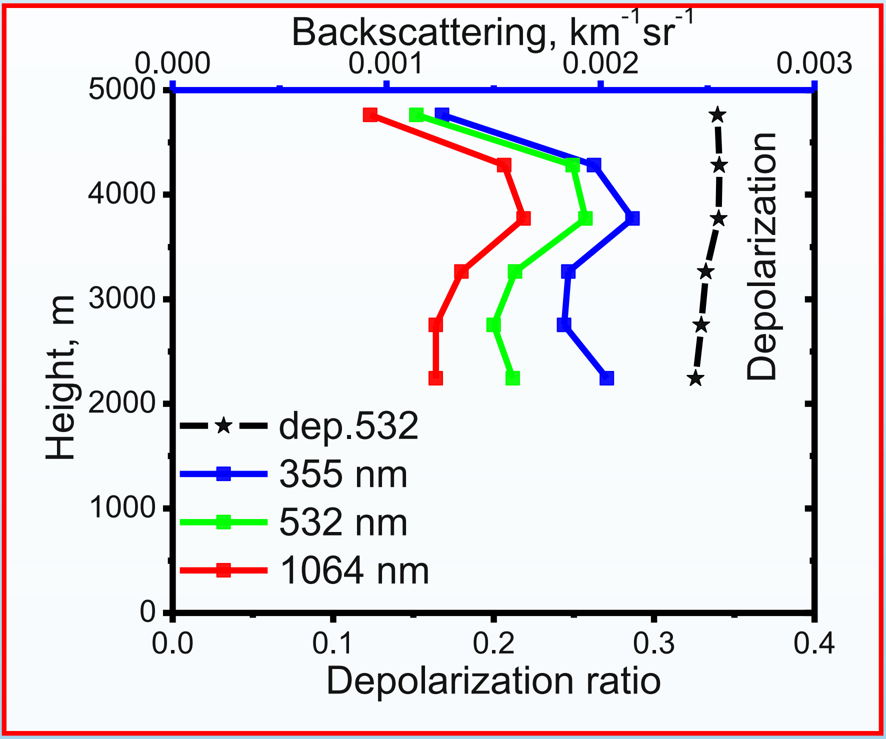

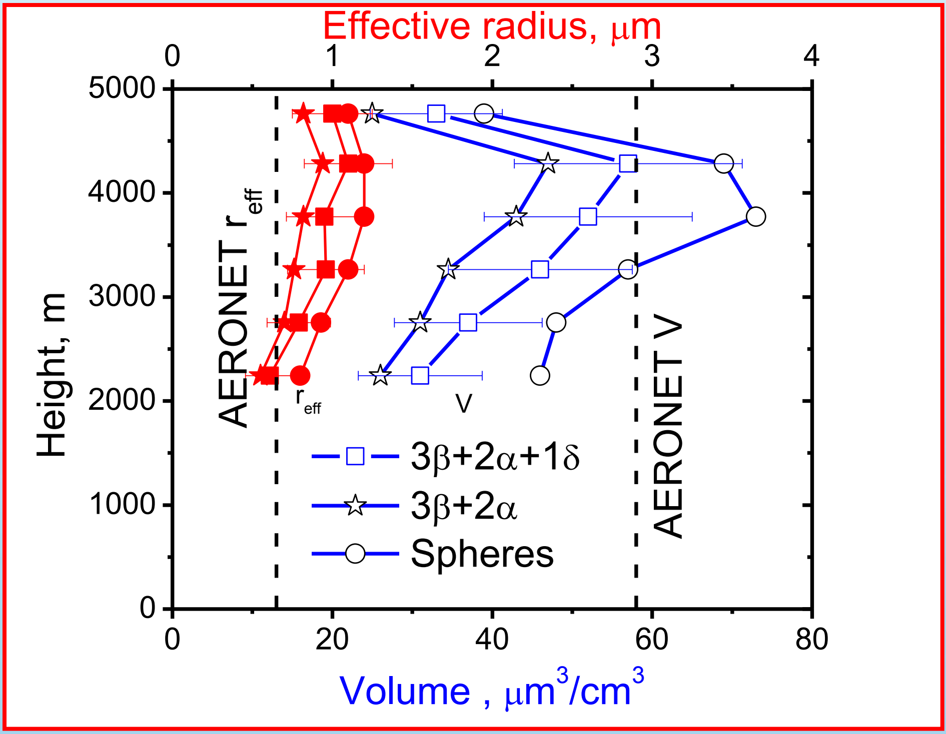

PSDs obtained from SAMUM-1 data

Optical data are provided by M.Tesche et al.

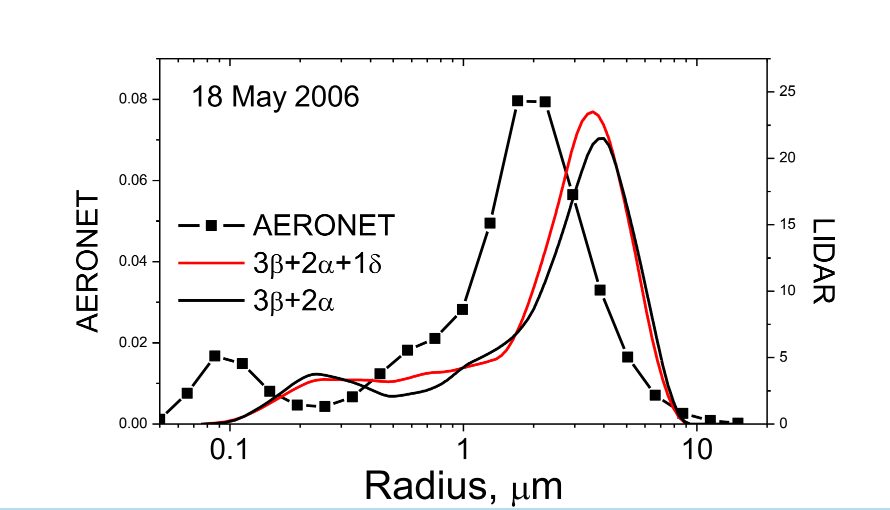

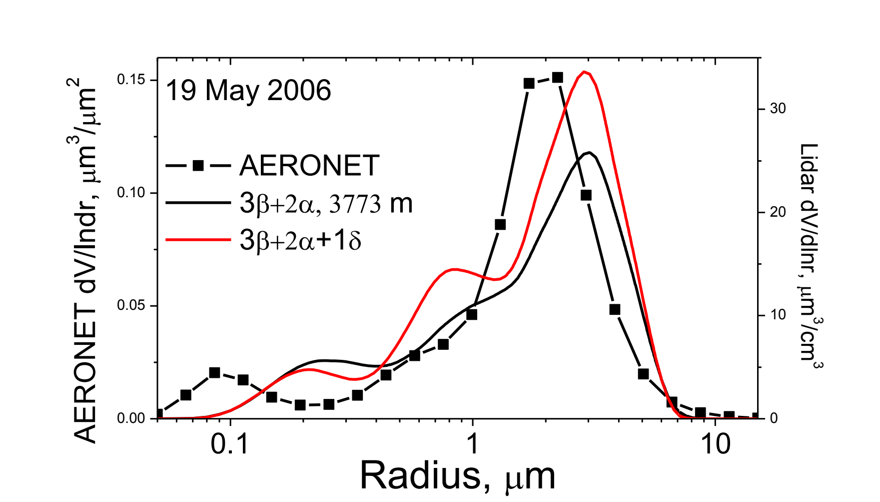

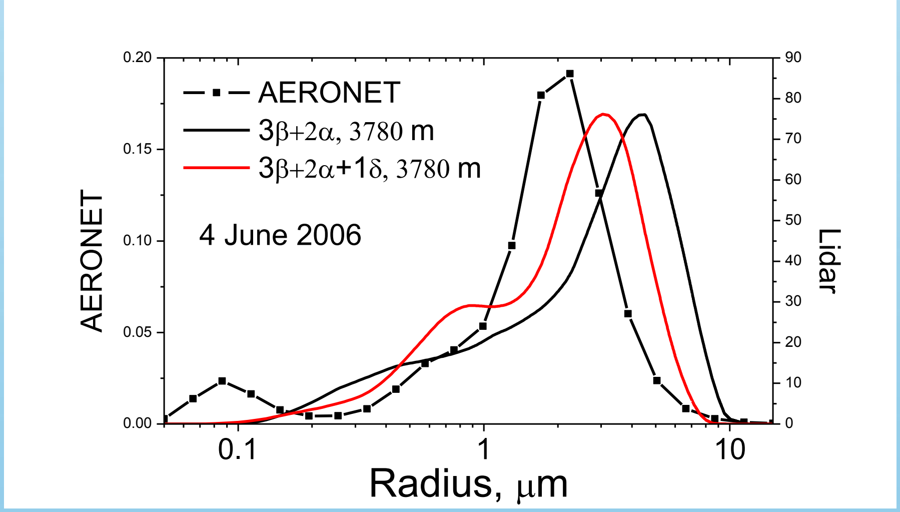

1. **Results obtained with and without depolarization are consistent.**
2. **AERONET provides lower values of effective radius.**
3. **Adding depolarization shifts PSD toward small radii**
4. **Lidar retrievals don't reveal the fine mode**
5. **AERONET provides lower values of the real part of refractive index.**

Retrieval of refractive index (May 19, 2006)

Optical data are provided by M.Tesche et al.

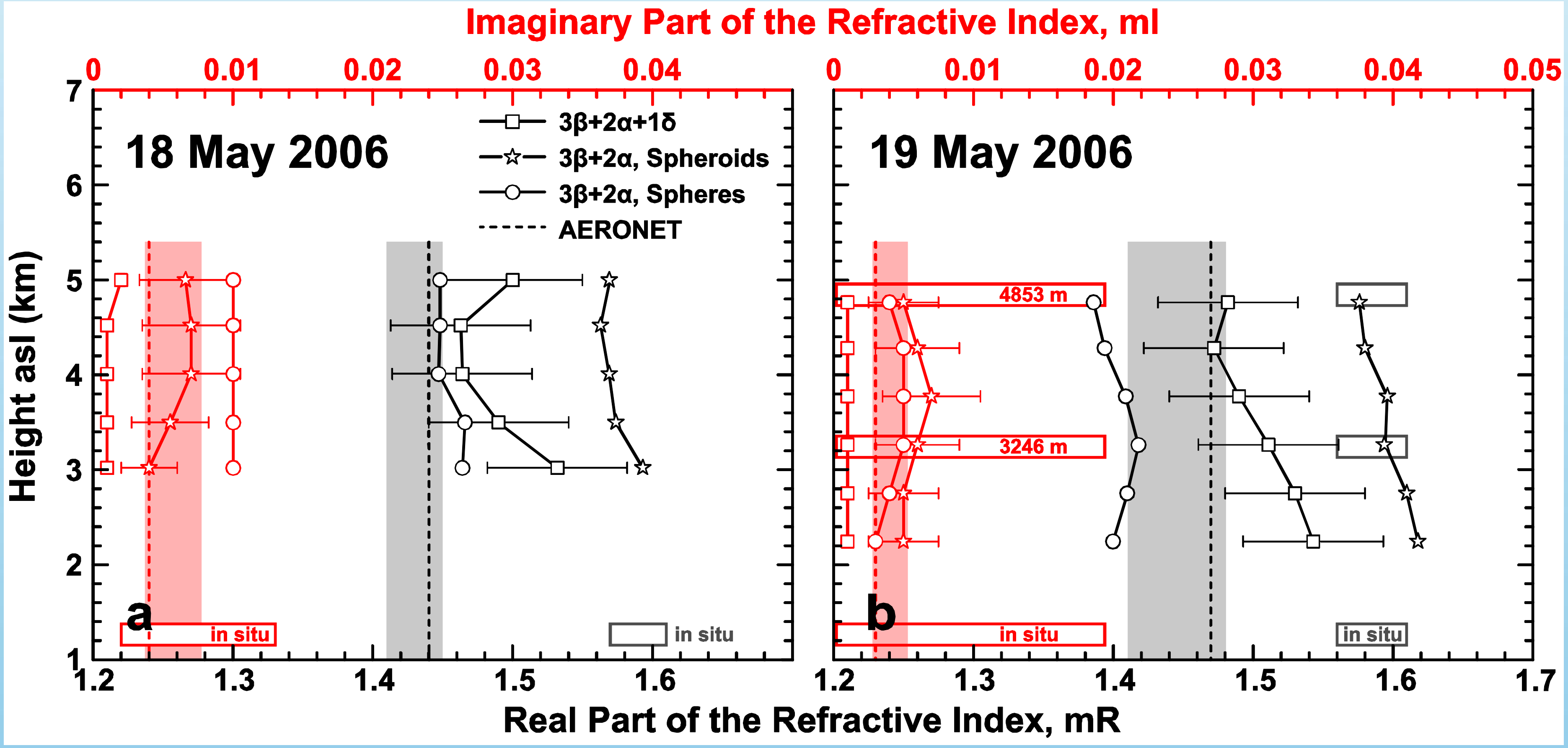

One of the issues is spectral dependence of particle refractive index

Spectral dependence of imaginary part of dust during SAMUM

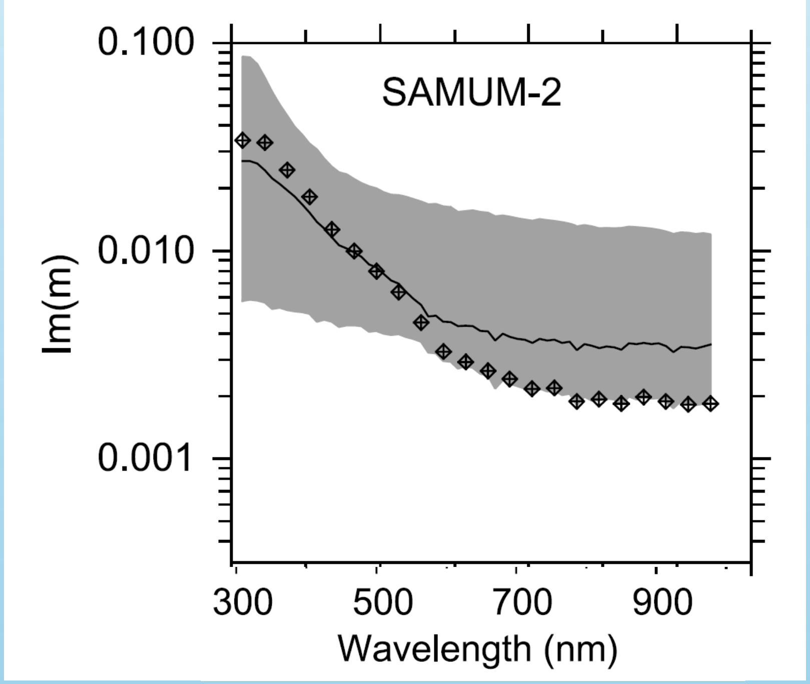

From Ansmann et al. 2011

Correction of Im spectral dependence in retrieval

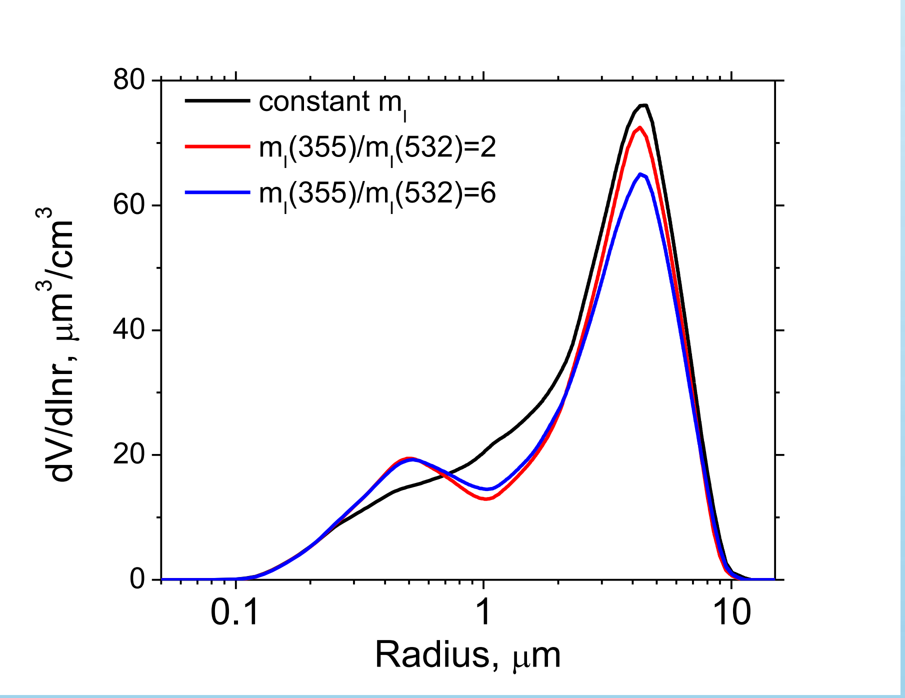

Optical data are provided by M.Tesche et al.
Details are given Veselovskii et al. JGR, 2010

Mixture of dust and smoke

SAMUM 2 (31 Jan 2008)

Tesche et al. JGR 2009

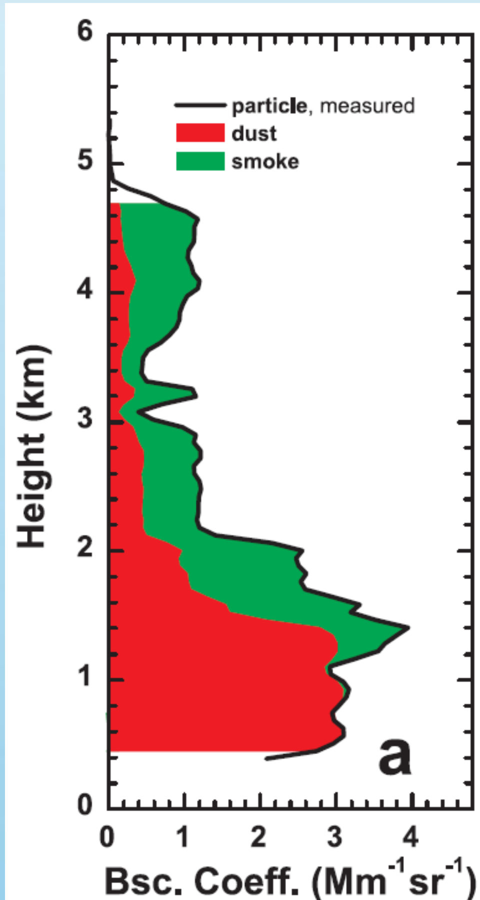

Optical data of Tesche et al. are used

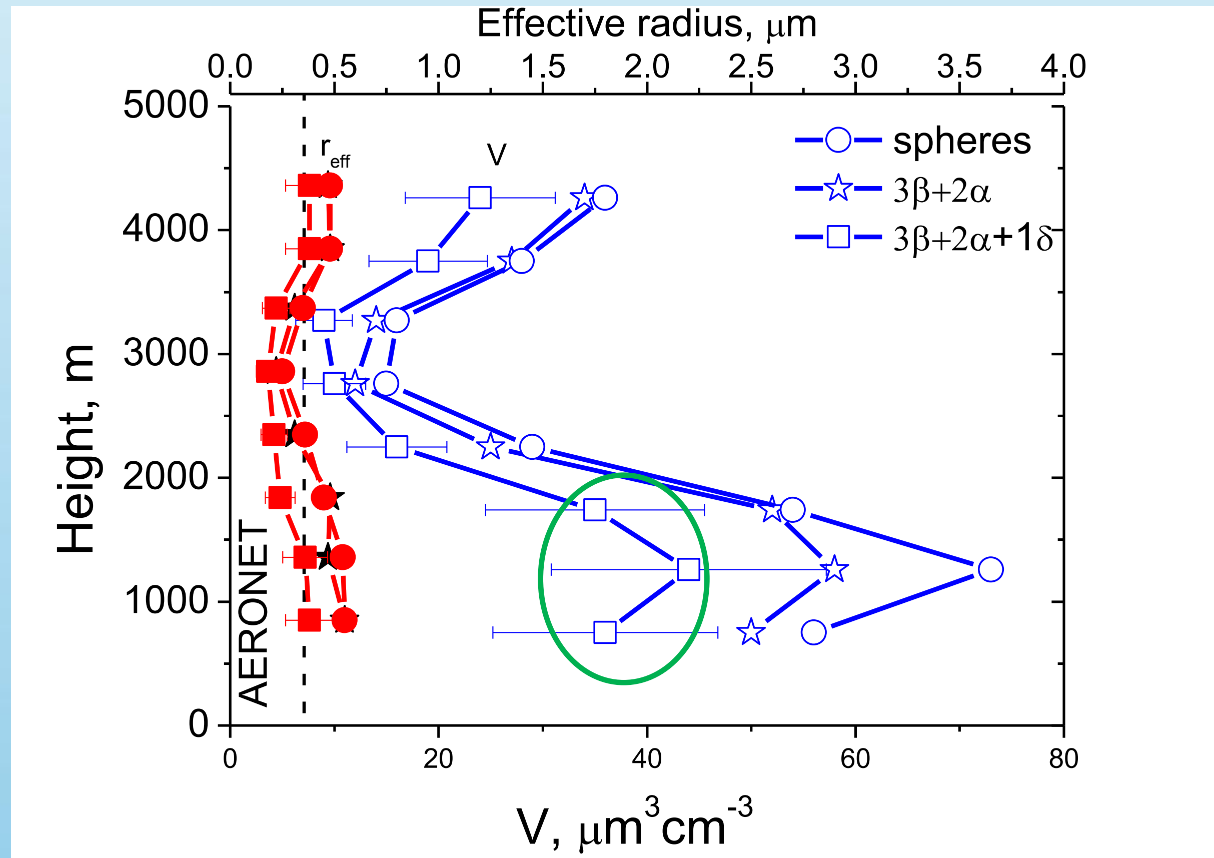

Optical data of Tesche et al. are used

Refractive index retrieval

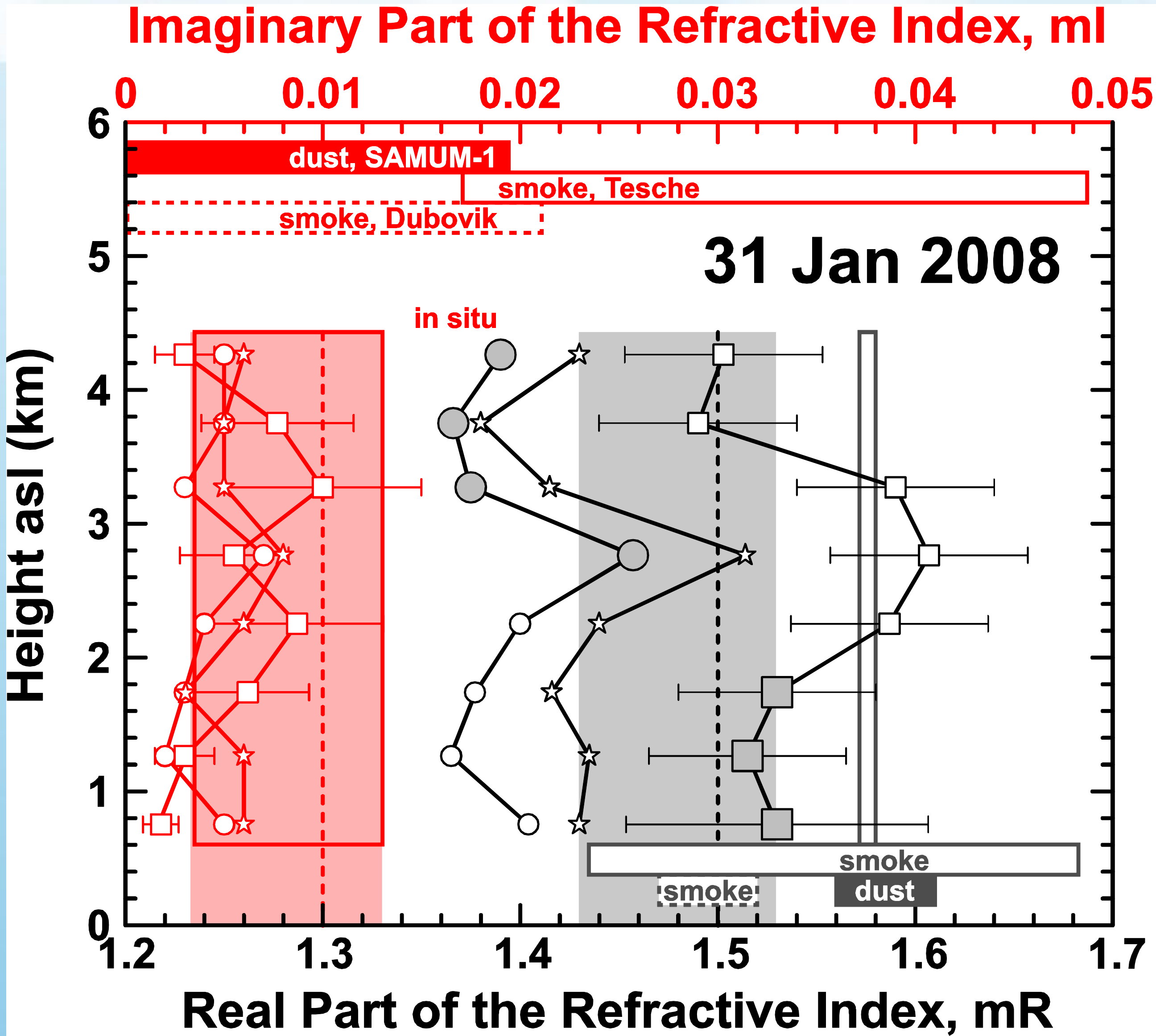

Conclusion

How many wavelengths do we need?

1λ + AERONET	**Particle concentration**
2λ + AERONET	**Profiles of effective radius and concentration (LIRIC)**
3λ	**For known refractive index – particle radii and concentration**
3+1	**For many cases – radii, concentration, RI**
3+2	**Particle size distribution, RI**
3+2+1δ	**Treatment of dust mixtures**
3+2+3δ	**Aerosol classification**

AERONET CIMEL SUN-PHOTOMETER

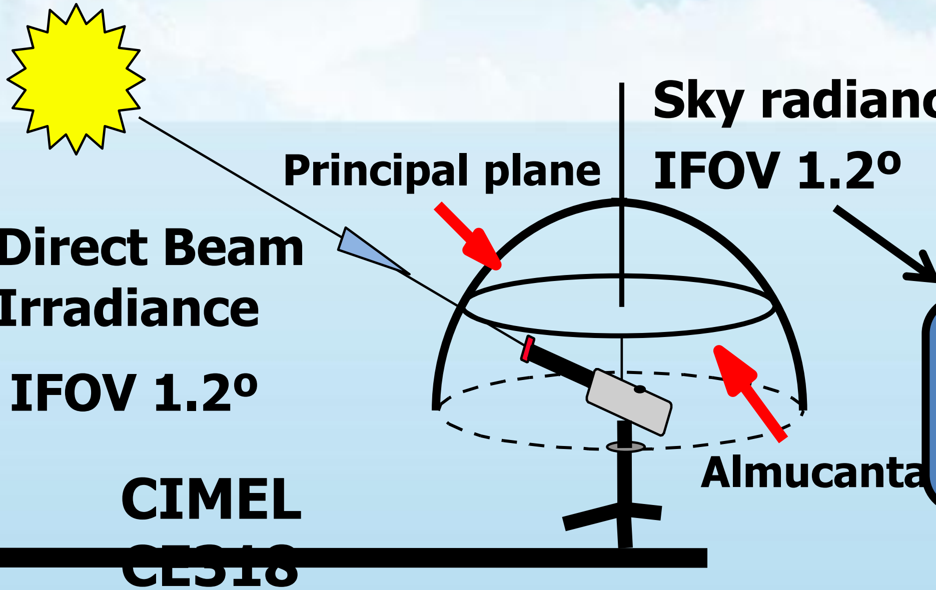

Retrieves aerosol optical depth (AOD) and sky radiances

Require symmetry and no clouds in the sky

Limited to large scattering angles (morning and afternoon)

Large amounts of measurements with other instruments that acquire only spectral AOD

Inversion scheme retrieves:

Size distribution (v(r)), Effective radius (r_{eff}) and V, S, N

Is able to separate absorption from scatting:

Aerosol refractive index ($m = m_r + im_i$) phase function P(Θ), asymmetry factor (g) and albedo (ω_0)

LINEAR ESTIMATION (LE)

Application to AERONET AOD(λ) measurements: Example

Good agreement between both methodologies for fine mode predominance

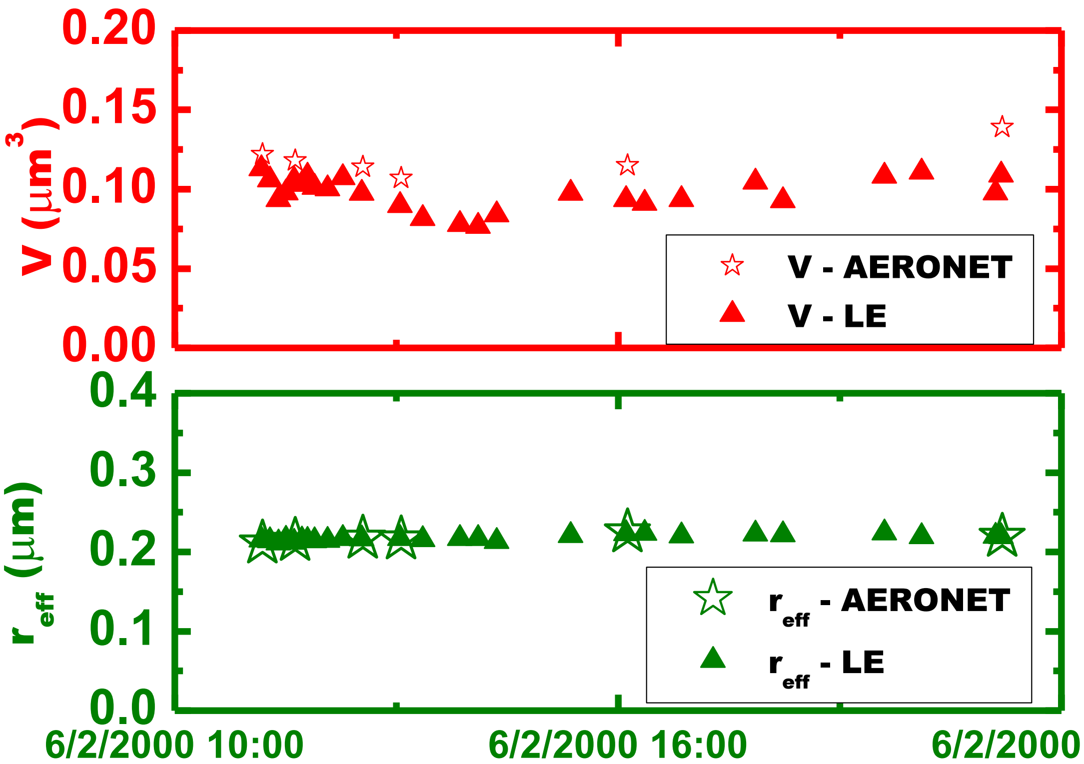

AERONET size distributions

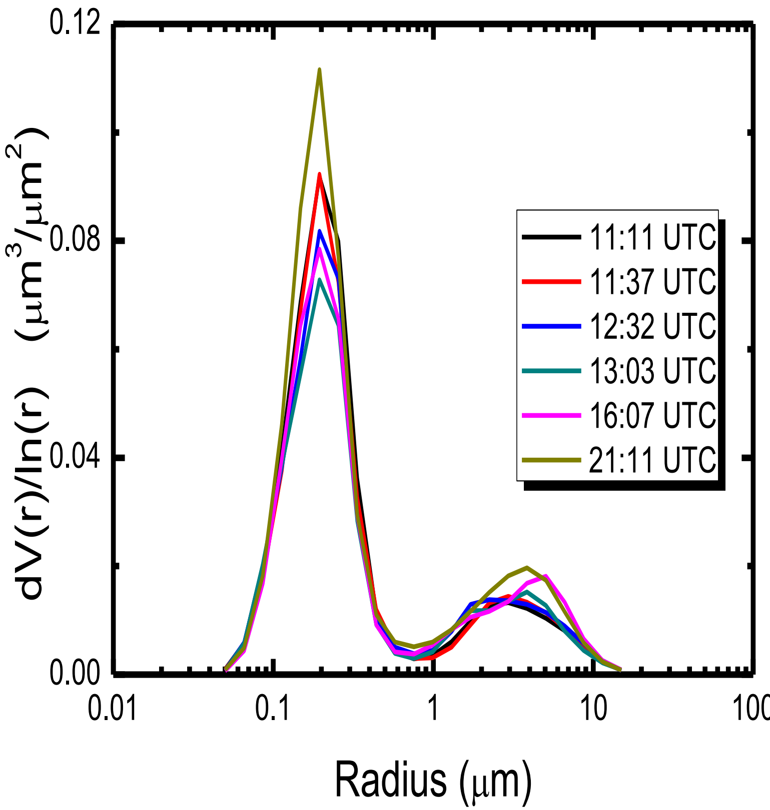

LINEAR ESTIMATION (LE)

Application to AERONET AOD(λ) measurements: Example

Relatively good agreement: Better temporal resolution using LE

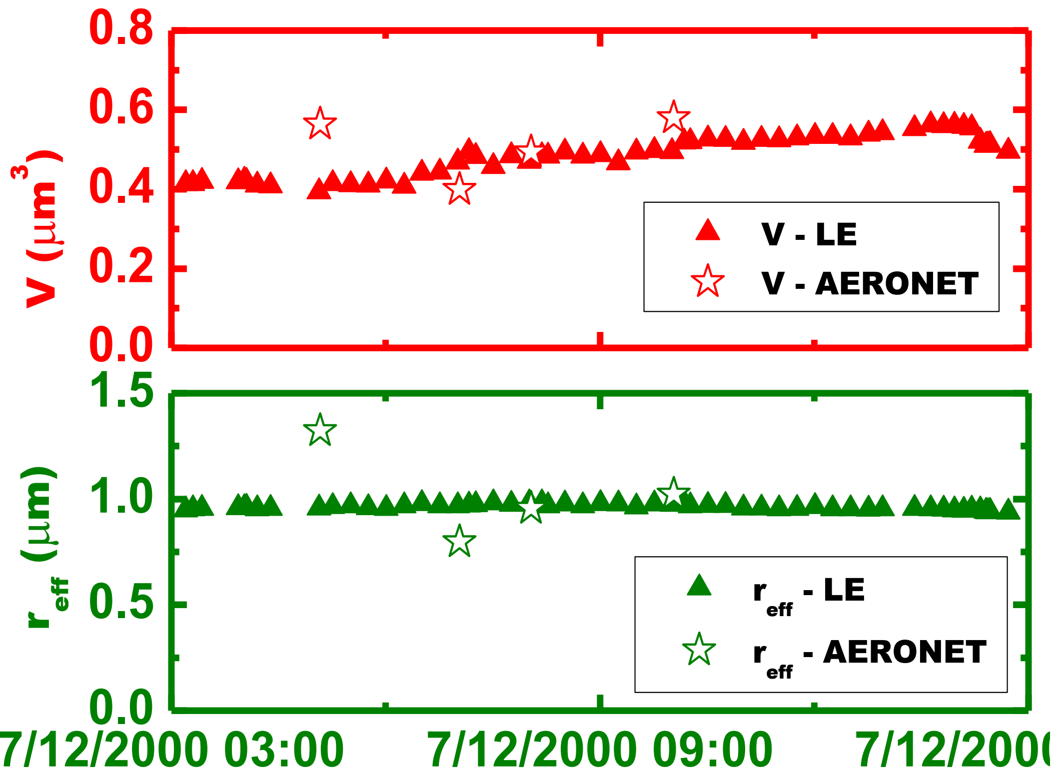

AERONET size distributions